Basic Concepts in Magnetism

J. M. D. Coey

School of Physics and CRANN, Trinity College Dublin

Ireland.

1. Magnetostatics
2. Magnetism of multi-electron atoms
3. Crystal field
4. Magnetism of the free electron gas
5. Dilute magnetic oxides

Comments and corrections please: jcoey@tcd.ie

www.tcd.ie/Physics/Magnetism

3. The Crystal Field

Summary so far

For free ions:

- Filled electronic shells are not magnetic. A ↑ and a ↓ electron is paired in each orbital.

- Only partly-filled shells may possess a magnetic moment.

- $\boldsymbol{m} = -g\mu_B \boldsymbol{J}/\hbar$. J is the total angular momentum quantum number given by Hund's rules. (This must be modified for ions in solids.)

- Orbital angular momentum for 3d ions is *quenched*. The spin-only magnetic moment is $\boldsymbol{m} = -(g\mu_B \boldsymbol{S}/\hbar)$, where g=2.

- Certain crystallographic directions become easy axes of magnetization- *magnetocrystalline anisotropy.*

$\Lambda(Co^{2+}) = -272$ K

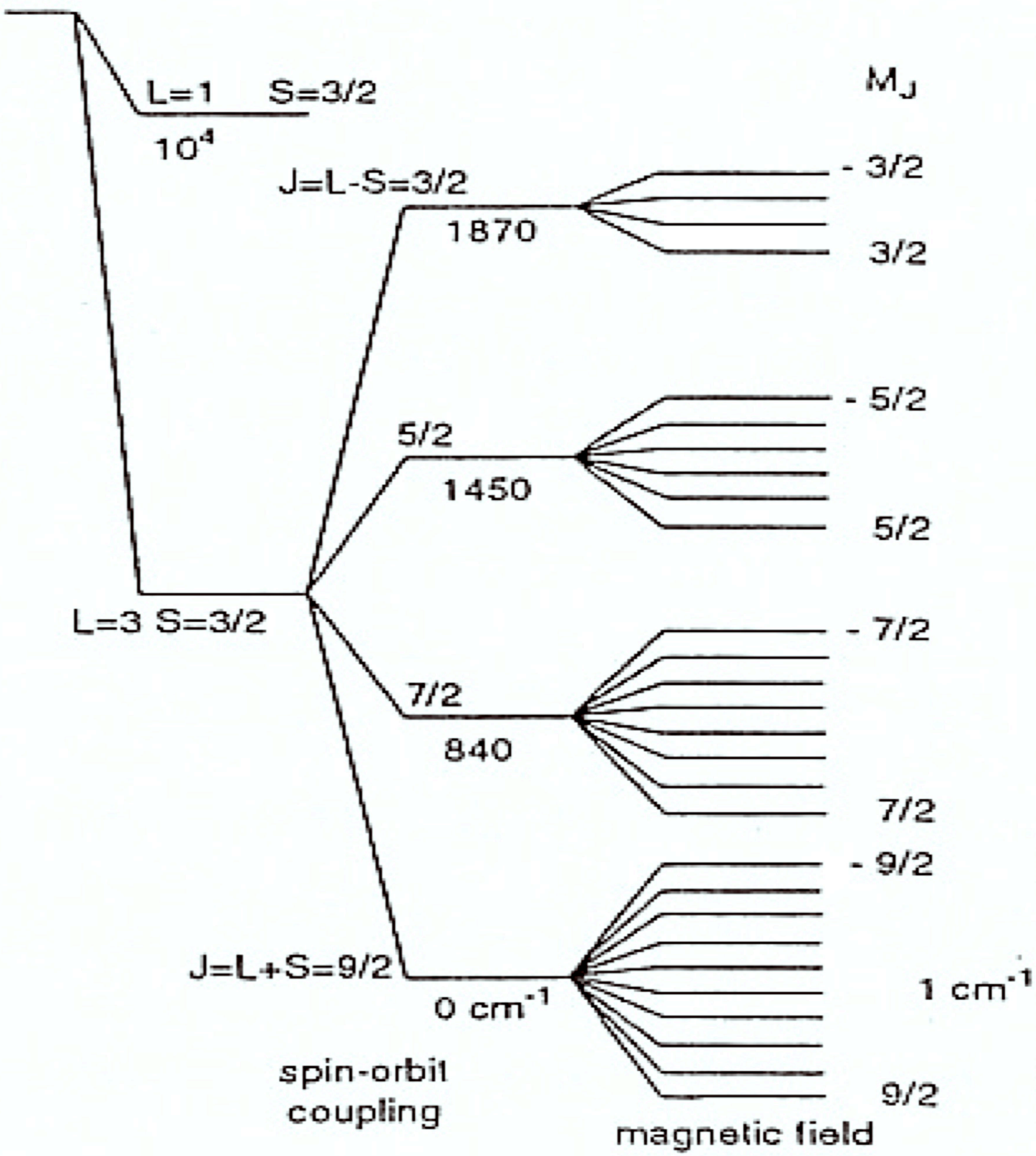

4f ions

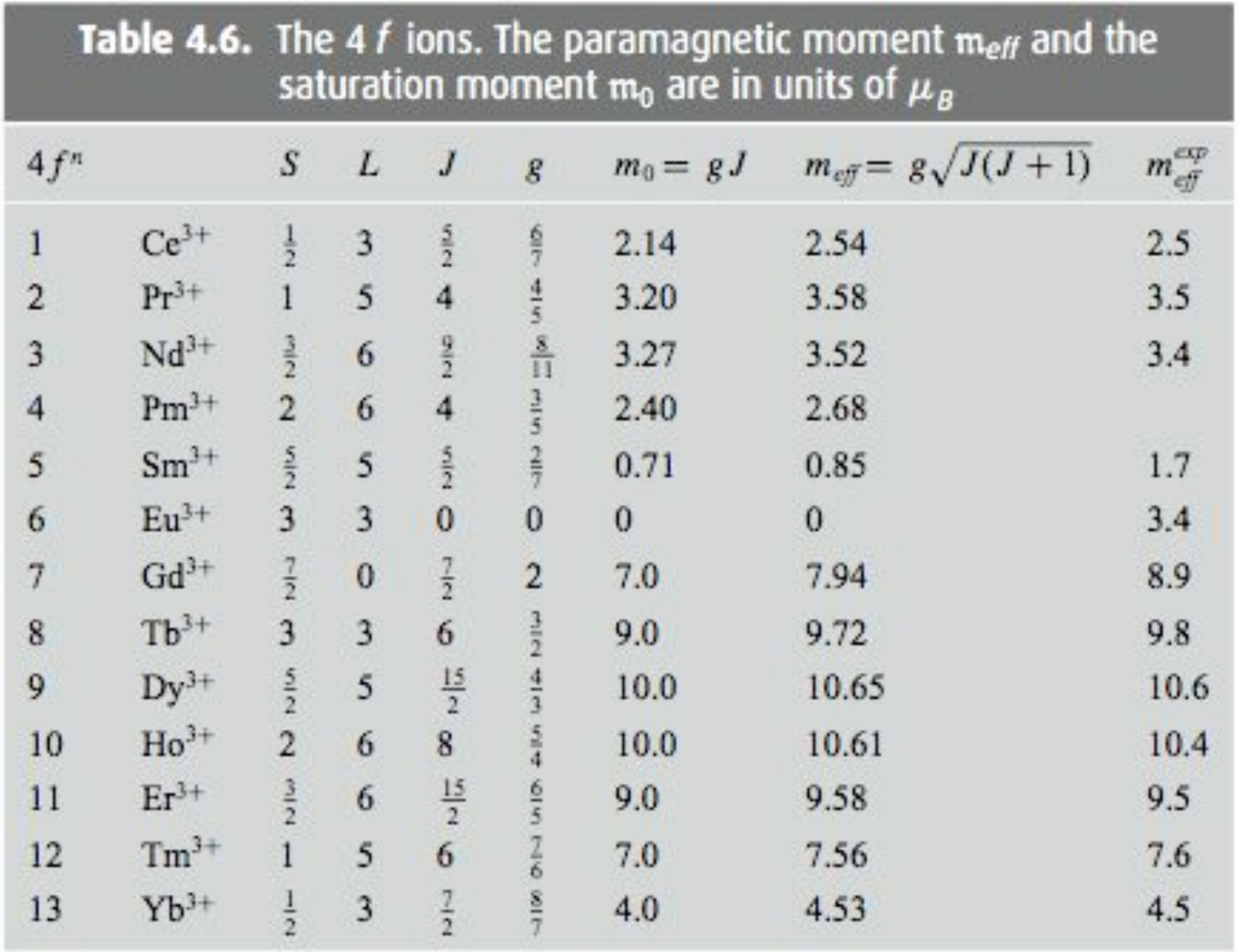

Table 4.6. The 4 *f* ions. The paramagnetic moment $\mathbf{m}_{eff}$ and the saturation moment $\mathbf{m}_0$ are in units of μ_B

$4f^n$		S	L	J	g	$m_0 = gJ$	$m_{eff} = g\sqrt{J(J+1)}$	m_{eff}^{exp}
1	Ce^{3+}	$\frac{1}{2}$	3	$\frac{5}{2}$	$\frac{6}{7}$	2.14	2.54	2.5
2	Pr^{3+}	1	5	4	$\frac{4}{5}$	3.20	3.58	3.5
3	Nd^{3+}	$\frac{3}{2}$	6	$\frac{9}{2}$	$\frac{8}{11}$	3.27	3.52	3.4
4	Pm^{3+}	2	6	4	$\frac{3}{5}$	2.40	2.68	
5	Sm^{3+}	$\frac{5}{2}$	5	$\frac{5}{2}$	$\frac{2}{7}$	0.71	0.85	1.7
6	Eu^{3+}	3	3	0	0	0	0	3.4
7	Gd^{3+}	$\frac{7}{2}$	0	$\frac{7}{2}$	2	7.0	7.94	8.9
8	Tb^{3+}	3	3	6	$\frac{3}{2}$	9.0	9.72	9.8
9	Dy^{3+}	$\frac{5}{2}$	5	$\frac{15}{2}$	$\frac{4}{3}$	10.0	10.65	10.6
10	Ho^{3+}	2	6	8	$\frac{5}{4}$	10.0	10.61	10.4
11	Er^{3+}	$\frac{3}{2}$	6	$\frac{15}{2}$	$\frac{6}{5}$	9.0	9.58	9.5
12	Tm^{3+}	1	5	6	$\frac{7}{6}$	7.0	7.56	7.6
13	Yb^{3+}	$\frac{1}{2}$	3	$\frac{7}{2}$	$\frac{8}{7}$	4.0	4.53	4.5

J is a good quantum number

3d ions

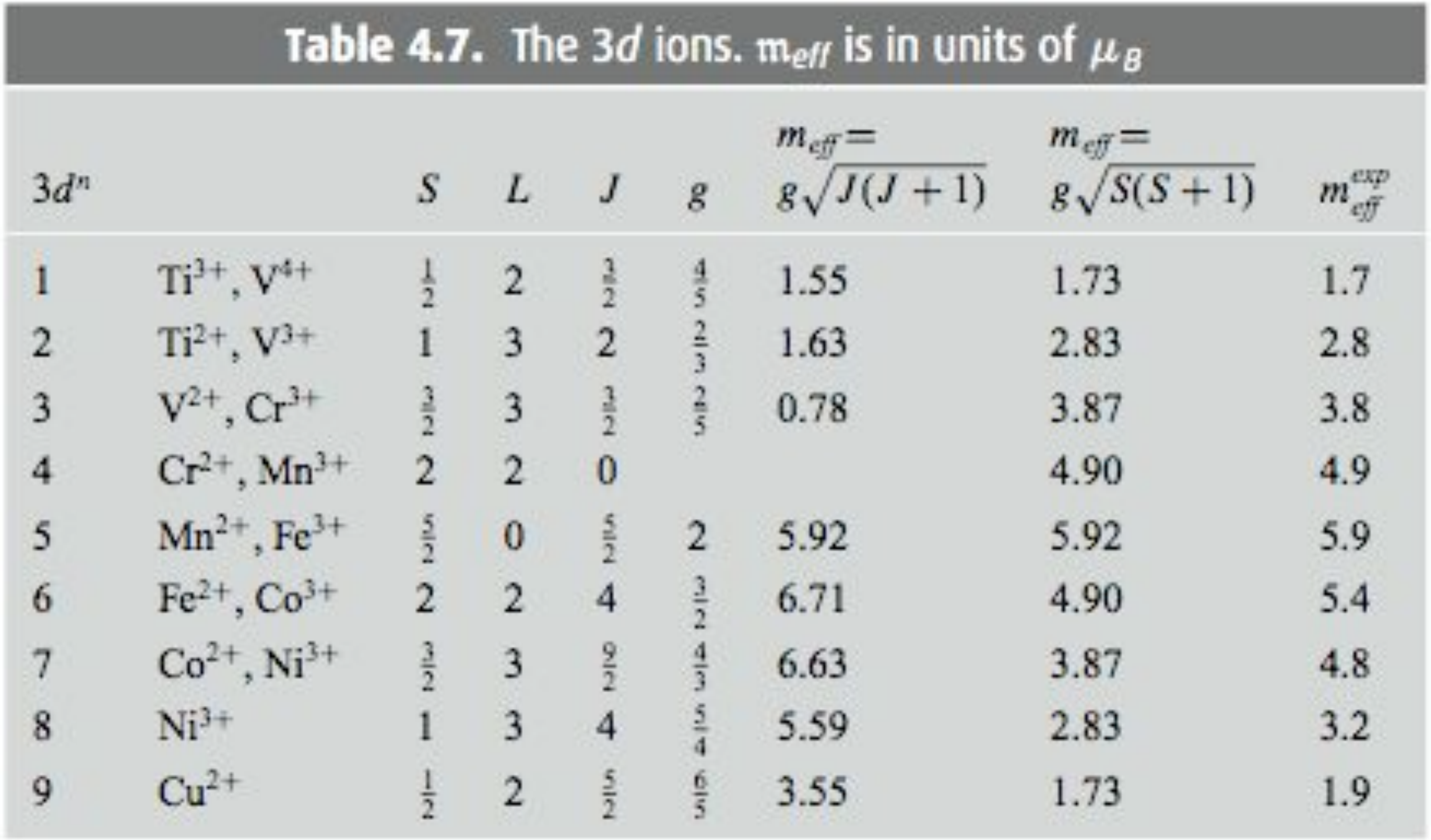

Table 4.7. The 3*d* ions. m_{eff} is in units of μ_B

$3d^n$		S	L	J	g	$m_{eff} = g\sqrt{J(J+1)}$	$m_{eff} = g\sqrt{S(S+1)}$	m_{eff}^{exp}
1	Ti^{3+}, V^{4+}	$\frac{1}{2}$	2	$\frac{3}{2}$	$\frac{4}{5}$	1.55	1.73	1.7
2	Ti^{2+}, V^{3+}	1	3	2	$\frac{2}{3}$	1.63	2.83	2.8
3	V^{2+}, Cr^{3+}	$\frac{3}{2}$	3	$\frac{3}{2}$	$\frac{2}{5}$	0.78	3.87	3.8
4	Cr^{2+}, Mn^{3+}	2	2	0			4.90	4.9
5	Mn^{2+}, Fe^{3+}	$\frac{5}{2}$	0	$\frac{5}{2}$	2	5.92	5.92	5.9
6	Fe^{2+}, Co^{3+}	2	2	4	$\frac{3}{2}$	6.71	4.90	5.4
7	Co^{2+}, Ni^{3+}	$\frac{3}{2}$	3	$\frac{9}{2}$	$\frac{4}{3}$	6.63	3.87	4.8
8	Ni^{3+}	1	3	4	$\frac{5}{4}$	5.59	2.83	3.2
9	Cu^{2+}	$\frac{1}{2}$	2	$\frac{5}{2}$	$\frac{6}{5}$	3.55	1.73	1.9

S is a good quantum number

3.1 The crystal field interaction

$$\mathcal{H}_i = \mathcal{H}_0 + \mathcal{H}_{so} \qquad + \mathcal{H}_Z$$

Coulomb interactions $|L,S\rangle$

spin-orbit interaction $\Lambda \boldsymbol{L}.\boldsymbol{S} \quad |J\rangle$

Zeeman interaction $g\boldsymbol{B}.\boldsymbol{J}\mu_B/\hbar \quad |M_J\rangle$

Crystal field interaction $\int \rho_0(\mathbf{r})\varphi_{cf}(r)d^3r$

	ion	Λ
$3d^1$	Ti^{3+}	124
$3d^2$	Ti^{2+}	88
$3d^3$	V^{2+}	82
$3d^4$	Cr^{2+}	85
$3d^6$	Fe^{2+}	-164
$3d^7$	Co^{2+}	-272
$3d^8$	Ni^{2+}	-493

$4f^1$	Ce^{3+}	920
$4f^2$	Pr^{3+}	540
$4f^3$	Nd^{3+}	430
$4f^5$	Sm^{3+}	350
$4f^8$	Tb^{3+}	-410
$4f^9$	Dy^{3+}	-550
$4f^{10}$	Ho^{3+}	-780
$4f^{11}$	Er^{3+}	-1170
$4f^{12}$	Tm^{3+}	-1900
$4f^{13}$	Yb^{3+}	-4140

	$\mathcal{H}_0$	$\mathcal{H}_{so}$	$\mathcal{H}_{cf}$	$\mathcal{H}_Z$ in 1 T
3d	1 - 5 10^4	10^2 -10^3	10^4	1
4f	1 - 6 10^5	1 - 5 10^3	$\approx 3\ 10^2$	1

Co

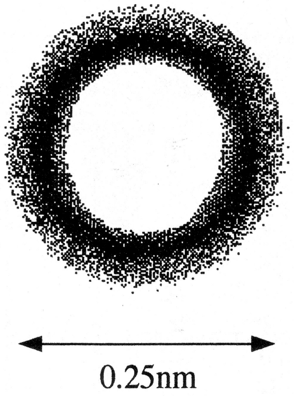

Gd

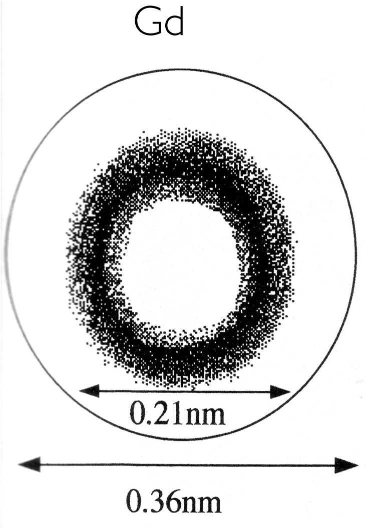

As metallic atoms, the transition metals occupy one third of the volume of the rare earths. As ions they occupy less than one tenth.

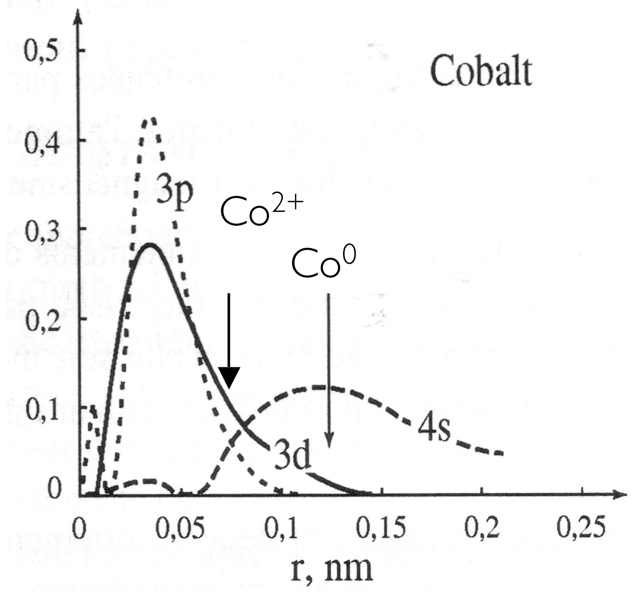

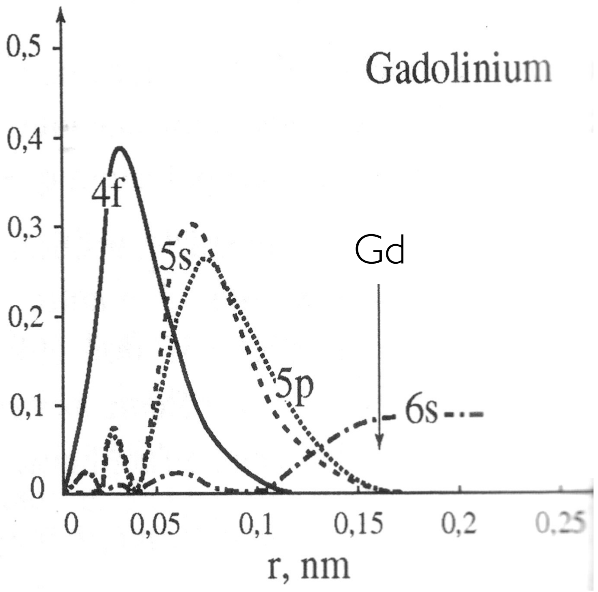

3.1.1 Ionic structures - oxides

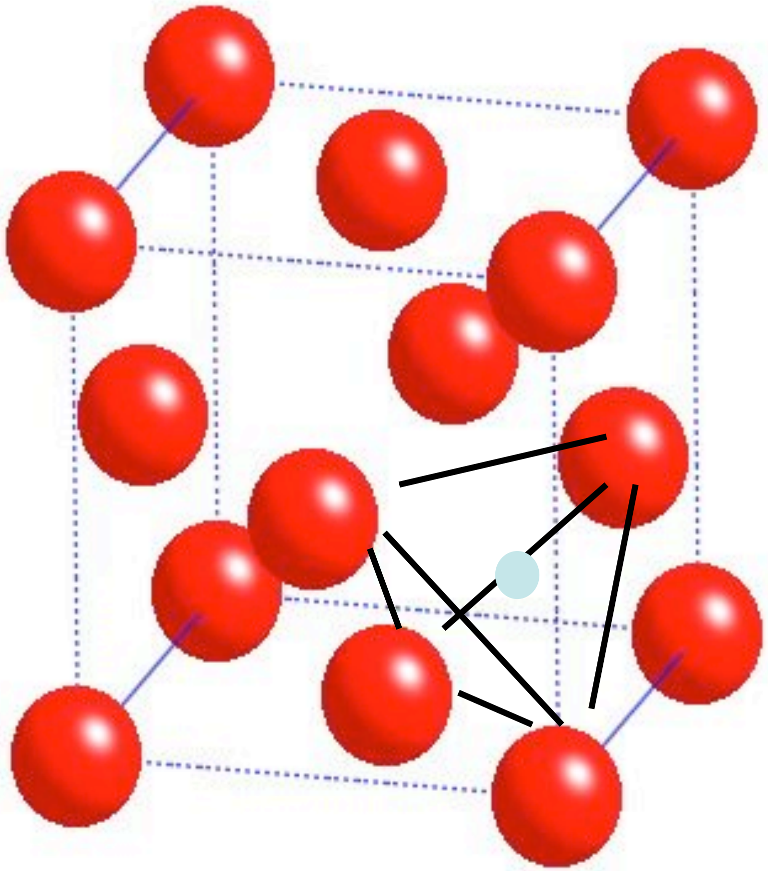

$R_{tet} = ((3/2)^{1/2} - 1)r_O \quad = 0.32$ pm

Cation radii in oxides: low spin values are in parentheses.

4-fold tetrahedral	pm	6-fold octahedral	pm	6-fold octahedral	pm	12-fold substitutional	pm
Mg^{2+}	53	Cr^{4+} $3d^2$	55	Ti^{3+} $3d^1$	67	Ca^{2+}	134
Zn^{2+}	60	Mn^{4+} $3d^3$	53	V^{3+} $3d^2$	64	Sr^{2+}	144
Al^{3+}	42			Cr^{3+} $3d^3$	62	Ba^{2+}	161
Fe^{3+} $3d^5$	52	Mn^{2+} $3d^5$	83	Mn^{3+} $3d^4$	65	Pb^{2+}	149
		Fe^{2+} $3d^6$	78 (61)	Fe^{3+} $3d^5$	64	Y^{3+}	119
		Co^{2+} $3d^7$	75 (65)	Co^{3+} $3d^6$	61 (56)	La^{3+}	136
		Ni^{2+} $3d^8$	69	Ni^{3+} $3d^7$	60	Gd^{3+}	122

The radius of the O^{2-} anion is 140 pm

3.2 One-Electron States - *d electrons*

Crystal fields and ligand fields

The most common coordination for 3d ions is 6-fold (octahedral) or 4-fold (tetrahedral). Both have cubi
symmetry, if undistorted. The crystal field can be estimated from a point-charge sum.

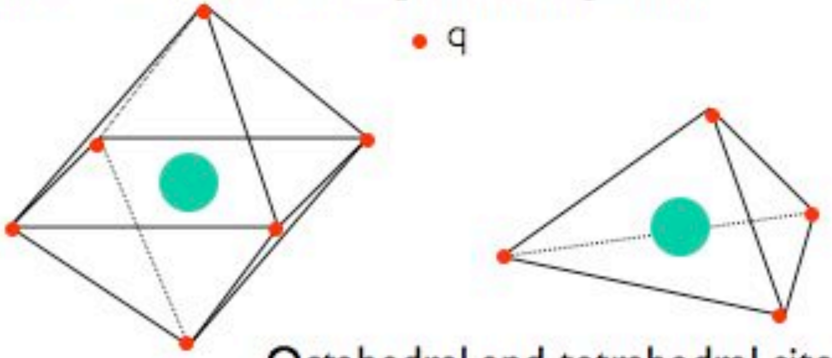

Octahedral and tetrahedral sites.

To demonstrate quenching of orbital angular momentum, we consider the l = 1 states $\psi^{0,}\ \psi^{1,}\ \psi^{-}$
corresponding to $m_l = 0, \pm 1$.

$$\psi^0 = R(r) \cos\theta$$

$$\psi^{\pm 1} = R(r) \sin\theta \exp\{\pm \iota\phi\}$$

The functions are eigenstates in the central potential V(r) but they are not eigenstates of $\mathcal{H}_{cf}$. Suppos
the oxygens can be represented by point charges q at their centres, then for the octahedron,

$$\mathcal{H}_{cf} = eV_{cf} = Dq(x^4 + y^4 + z^4 - 3y^2z^2 - 3z^2x^2 - 3x^2y^2)$$

where $D \approx e/4pe_o a^6$. But $\psi^{\pm 1}$ are *not* eigenfunctions of $V_{cf,}$ e.g. $\int \psi_i^* V_{cf} \psi^j dV \neq \delta_{ij}$, where i,j = -1, 0, 1.
We seek linear combinations that are eigenfunctions, namely

$$\psi^0 = R(r) \cos\theta = zR(r) = p_z$$

$$(1/\sqrt{2})(\psi^1 + \psi^{-1}) = R'(r)\sin\theta\cos\phi = xR(r) = p_x$$

s, p and d orbitals in the crystal field

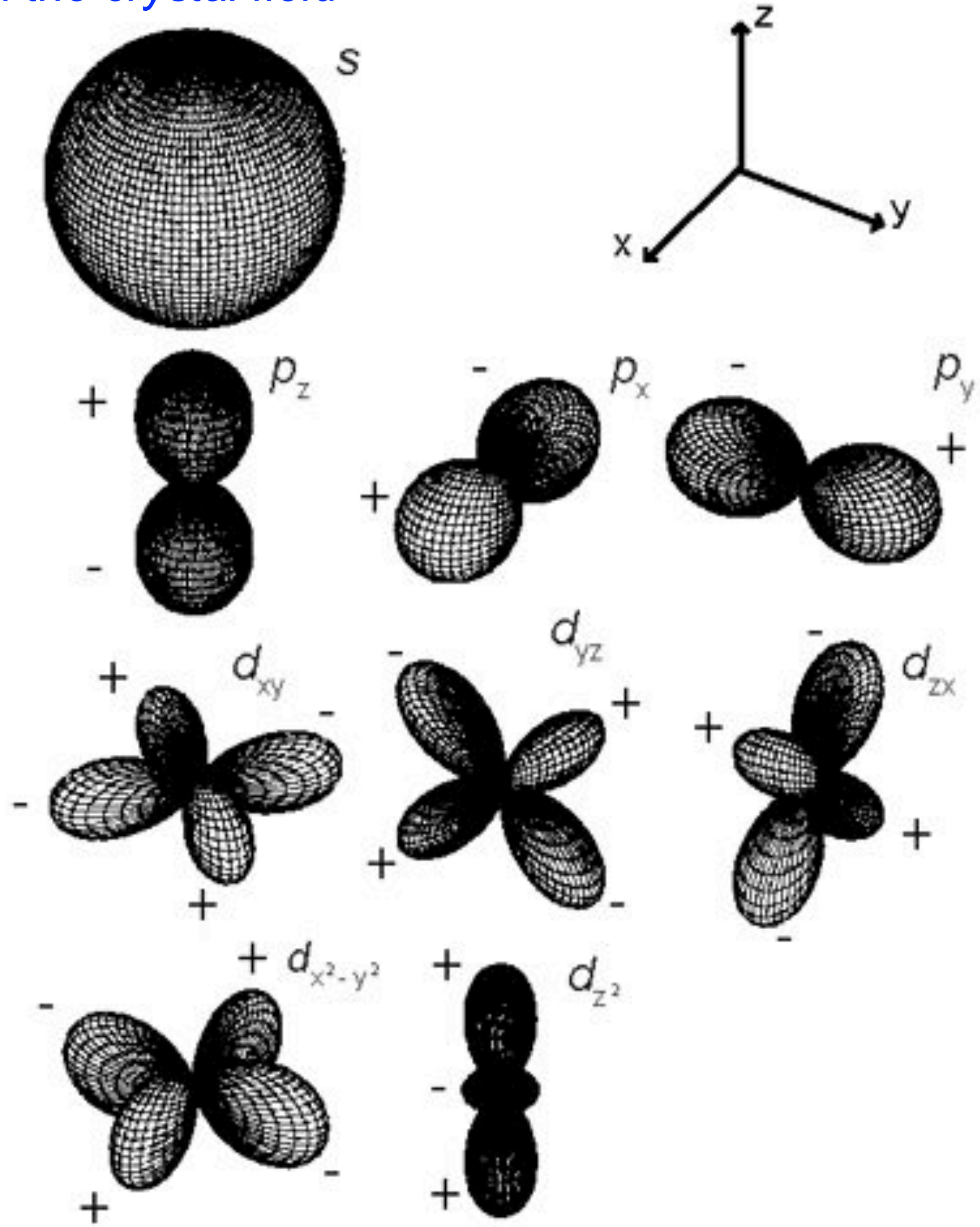

Orbitals in the crystal field

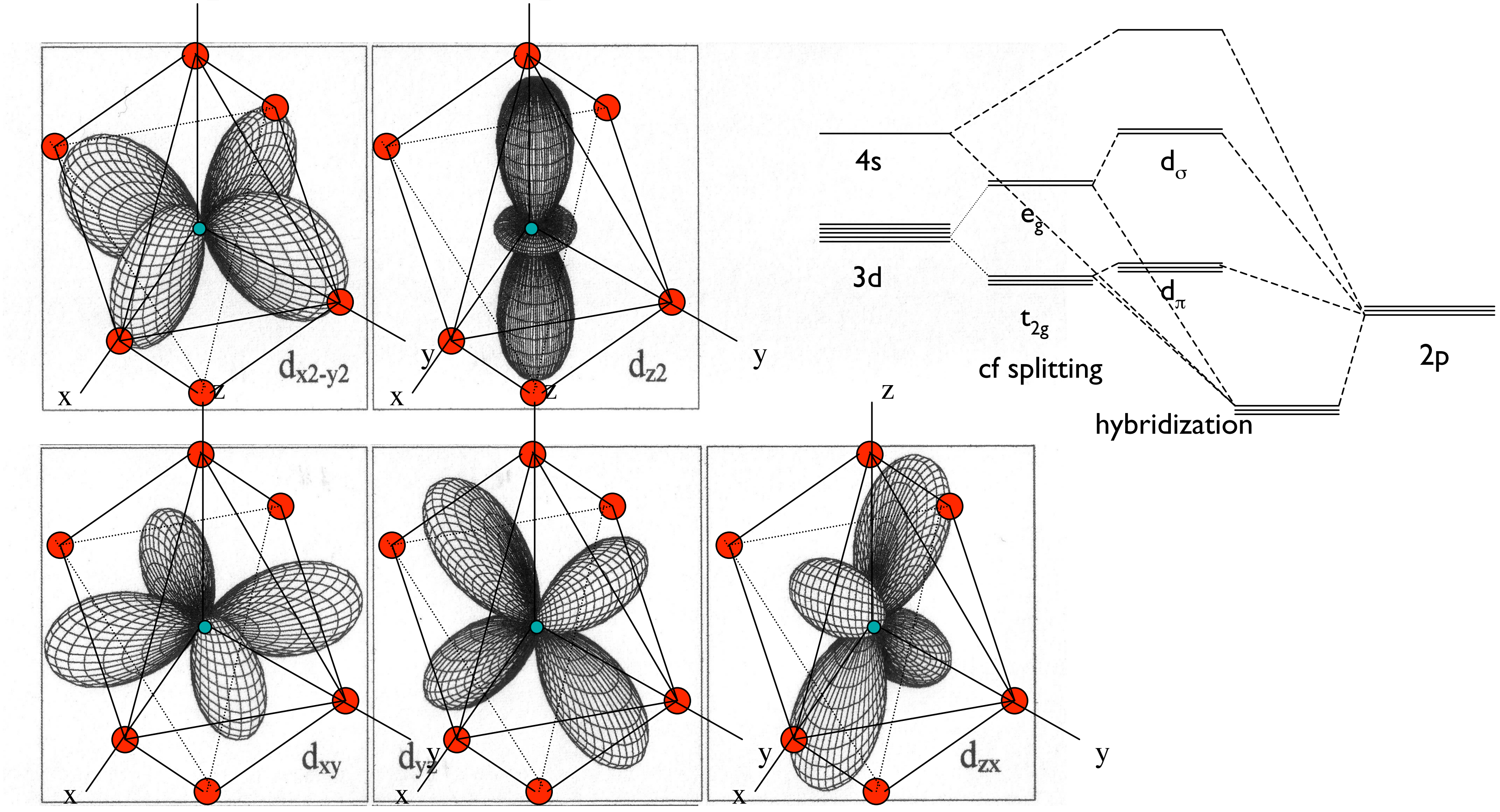

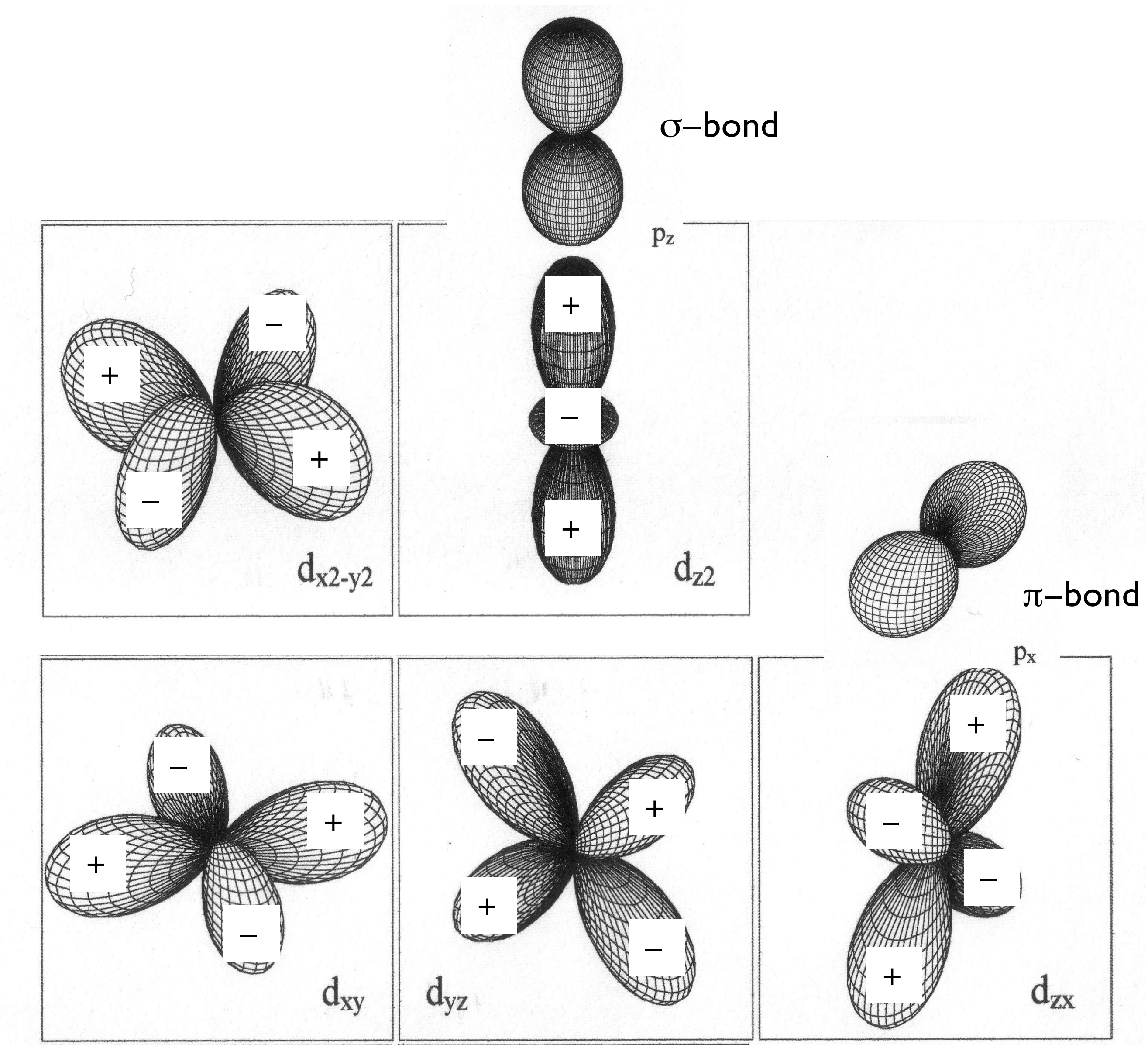

σ–bond

π–bond

+

Note that the z-component of angular momentum; $l_z\hbar = i\hbar\partial/\partial\phi$ is *zero* for these wavefunctions. Hen
the orbital angular momentum is quenched.

The same applies to 3d orbitals; the eigenfunctions there are

$$d_{xy} = (1/\sqrt{2})(\psi^2 - \psi^{-2}) = \quad R'(r)\sin^2\theta\sin2\phi \quad \approx xyR(r)$$
$$d_{yz} = (1/\sqrt{2})(\psi^1 - \psi^{-1}) = \quad R'(r)\sin\theta\cos\theta\sin\phi \quad \approx yzR(r) \qquad t_{2g}\ \textit{orbitals}$$
$$d_{zx} = (1/\sqrt{2})(\psi^1 + \psi^{-1}) = \quad R'(r)\sin\theta\cos\theta\cos\phi \quad \approx zxR(r)$$
$$d_{x^2-y^2} = (1/\sqrt{2})(\psi^2 + \psi^{-2}) = \quad R'(r)\sin^2\theta\cos2\phi \quad \approx (x^2-y^2)R(r) \qquad e_g\ \textit{orbitals}$$
$$d_{3z^2-r^2} = \psi^0 \quad = \quad R'(r)(3\cos^2\theta - 1) \quad \approx (3z^2-r^2)R(r)$$

The three p-orbitals are degenerate in a cubic crystal field, whether octahedral or tetrahedral, whereas the five d-orbitals split into a group of three t_{2g} and a group of two e_g orbitals

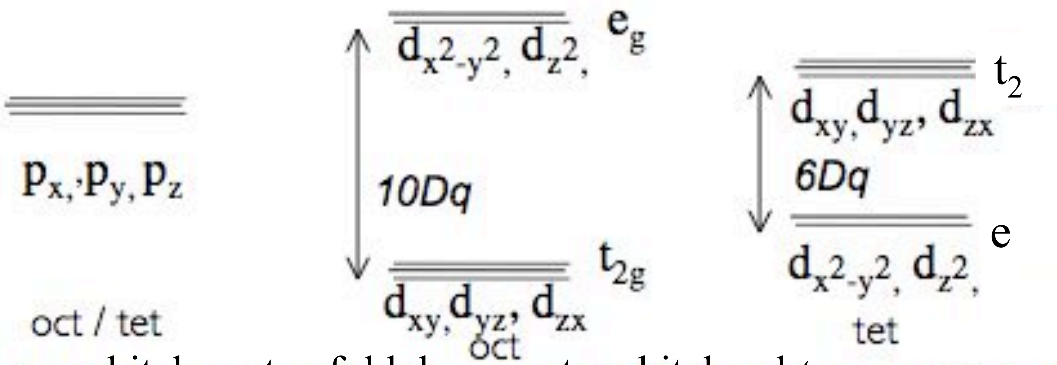

Notation: *a* or *b* denote a non-degenerate electron orbital, *e* a twofold degenerate orbital and *t* a threefold degenerate orbital. Capital letters refer to multi-electron states. a, *A* are non-degenerate and symmetric with respect to the principal axes of symmetry (the sign of the wavefunction is unchanged), *b* and *B* are antisymmetric with respect to the principal axis (the sign of the wavefunction changes). Subscripts *g* and *u* indicate whether the wavefunction is symmetric or antisymmetric under inversion. 1 refers to the mirror planes parallel to a symmetry axis and 2 refers to diagonal mirror planes.

Crystal-field theory regards the splitting of the 3d orbitals in octahedral oxygen, for example, as an electrostatic interaction with neighbouring point charges (oxygen anions). In reality the 3d and 2p orbitals of oxygen overlap to form a partially covalent bond. The oxygens bonding to the 3d metals are the *ligands*. The overlap is greater for the e_g than the t_{2g} orbitals in octahedral coordination.

The overlap leads to mixed wavefunctions, producing bonding and antibonding orbitals, whose splitting increases with overlap. The hybridized orbitals are

$$\phi = \alpha\psi_{2p}+\beta\psi_{3d}$$

where $\alpha^2+\beta^2=1$.

For 3d ions the splitting is usually 1-2eV, with the ionic and covalent contributions being of comparable magnitude

The *spectrochemical series* is the sequence of ligands in order of effectiveness at producing crystal/ligand field splitting.

$$Br^-<Cl^-<F^-<OH^-<CO^{2-}_3<O^{2-}<H_20<NH_3<SO^{2-}_3<NO^-_2<S^{2-}<CN^-$$

The bond is mostly ionic at the beginning of the series and covalent at the end.

Covalency is stronger in tetrahedral coordination but the crystal field splitting is

$$\Delta_{tet}=(3/5)\Delta_{oct}$$

3.2.1 Electronic structure of oxides

The 3d shell typically has integral occupancy $3d^n$. The 3d band is narrow, and lies in the 2p(O) -4s(M) gap 2 – 6 eV. The Fermi level lies in the d-band.

Is the oxide a conductor or an insulator ?

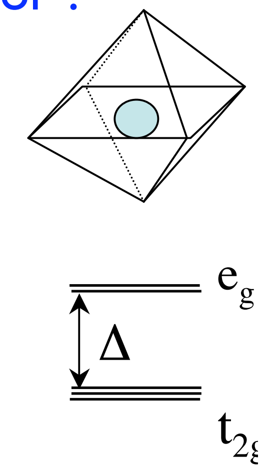

Mott pointed out that for a metal, it is necessary to have some ions in $3d^{n+1}$ and $3d^{n-1}$ states. This is only feasable if the bandwidth W is wide enough. i.e. $W > U_{mott}$ where U_{mott} is (ionization energy - electron affinity). If $W < U_{mott}$ we have a *Mott insulator*

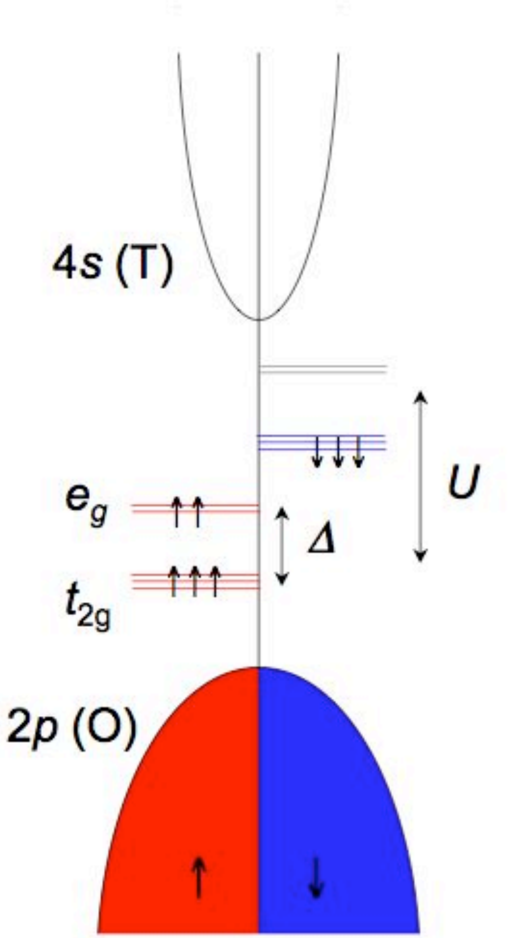

Example NiO

3.2.2 One-electron energy diagrams

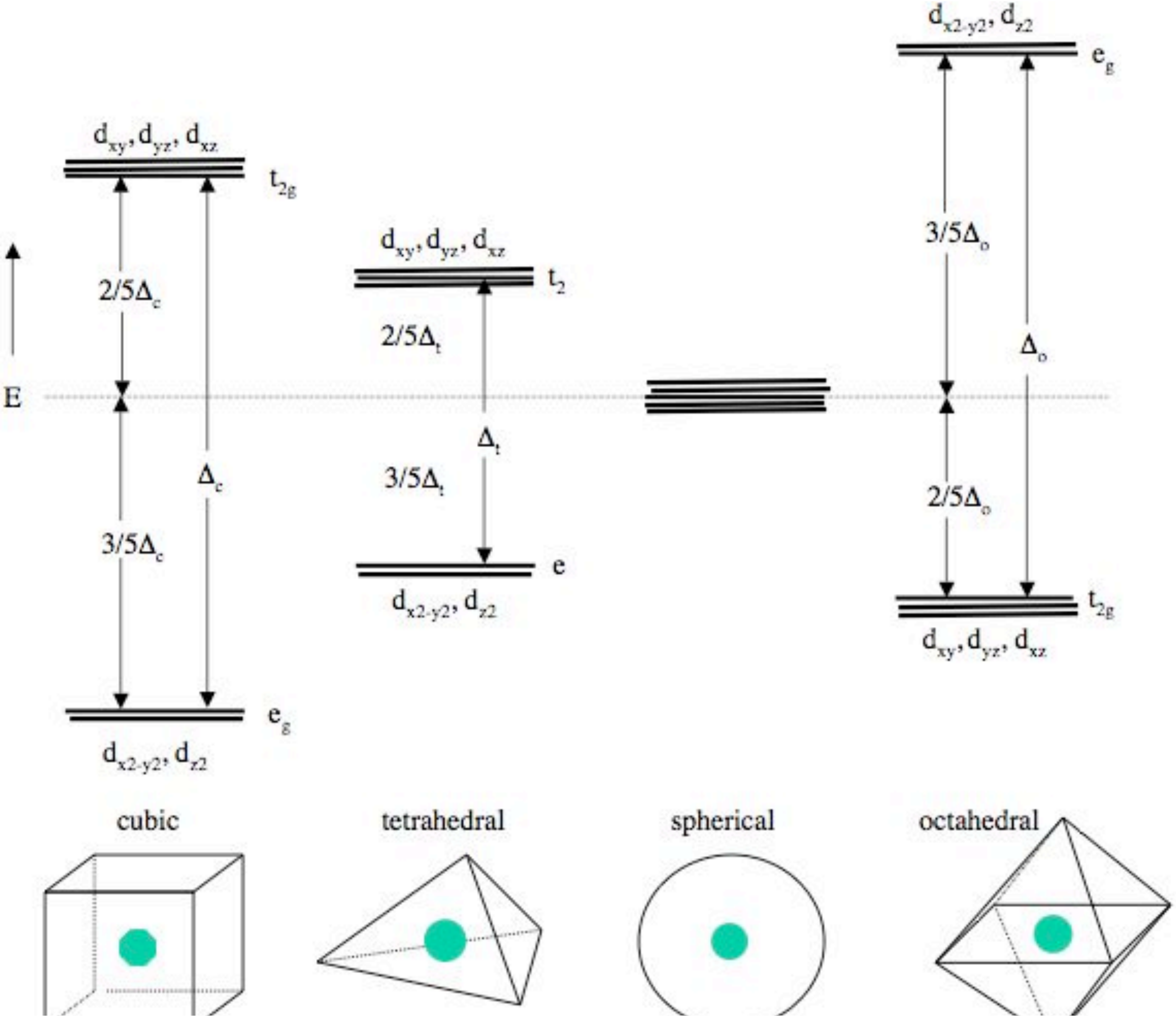

Lower symmetry

As the site symmetry is reduced, the degeneracy of the one-electron energy levels is raised. For example, a tetragonal extension of the octahedron along the z-axis will lower p_z and raise p_x and p_y. The effect on the d-states is shown below. The degeneracy of the d-levels in different symmetry is shown in the table.

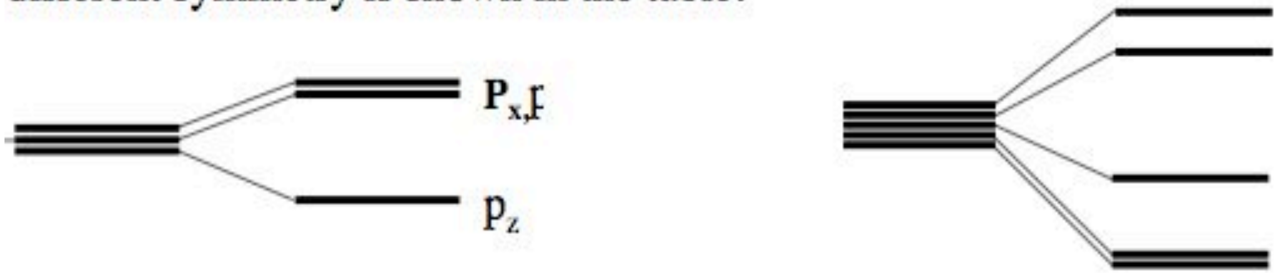

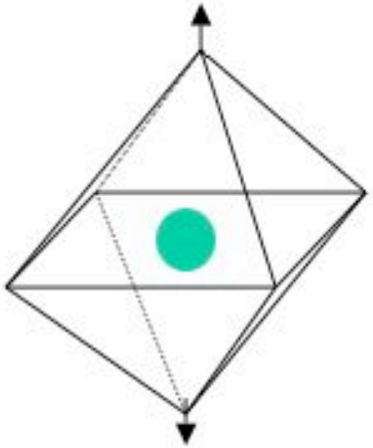

The effect of a tetragonal distortion of octahedral symmetry on the one-electron energy levels.

The splitting of the 1-electron levels in different symmetry

.

	l	Cubic	Tetragonal	Trigonal	Rhombohedral
s	**1**	**1**	**1**	**1**	**1**
p	**2**	**3**	**1,2**	**1,2**	**1,1,1**
d	**3**	**2,3**	**1,1,1,2**	**1,2,2**	**1,1,1,1,1**
f	**4**	**1,3,3**	**1,1,1,2,2**	**1,1,1,2,2**	**1,1,1,1,1,1,1**

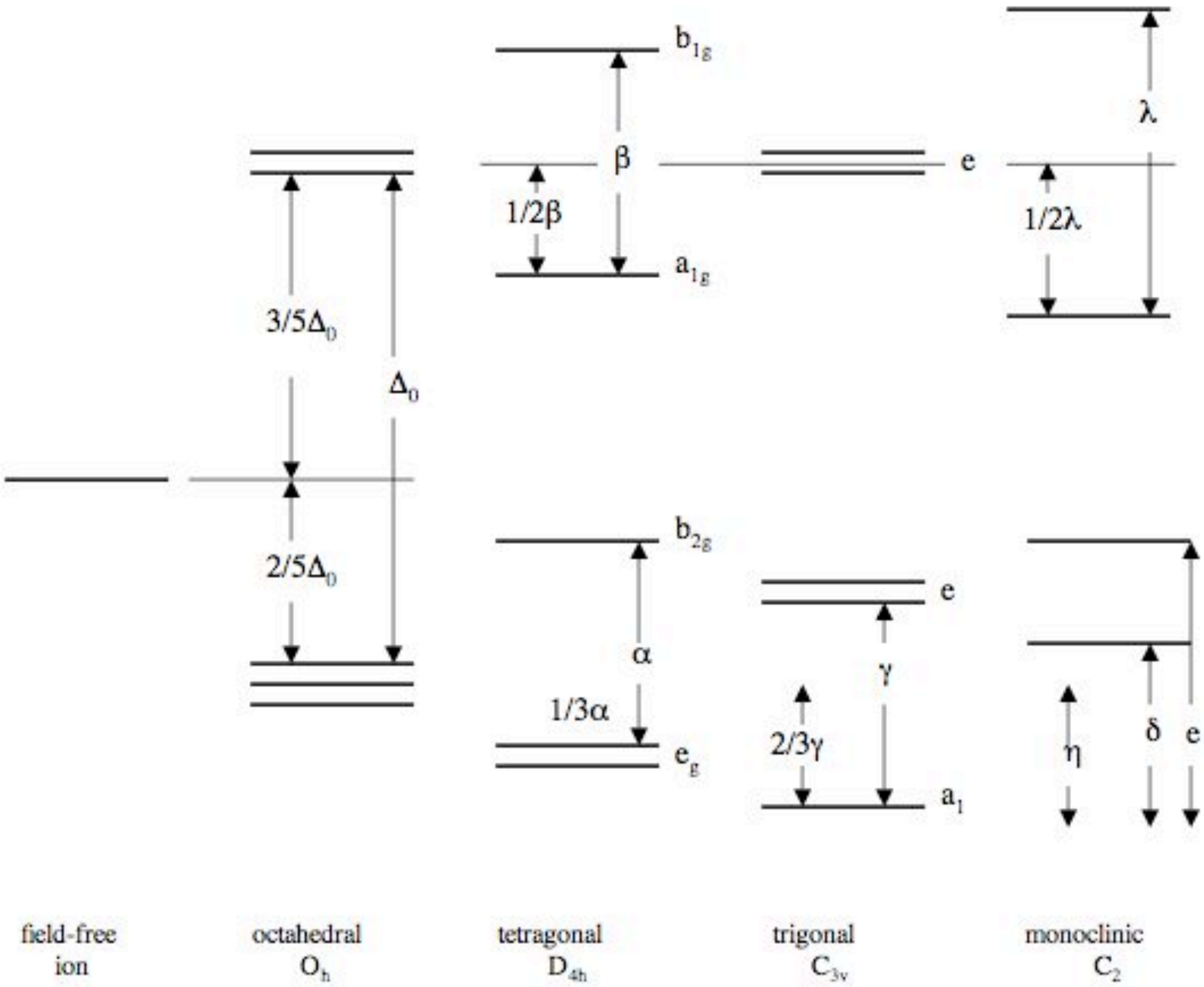

b1g
β
1/2β
a1g
e
λ
1/2λ
3/5Δ0
Δ0
2/5Δ0
b2g
α
1/3α
eg
e
γ
2/3γ
a1
η
δ
e
field-free
ion
octahedral
Oh
tetragonal
D4h
trigonal
C3v
monoclinic
C2

3.2.2 The Jahn-Teller effect

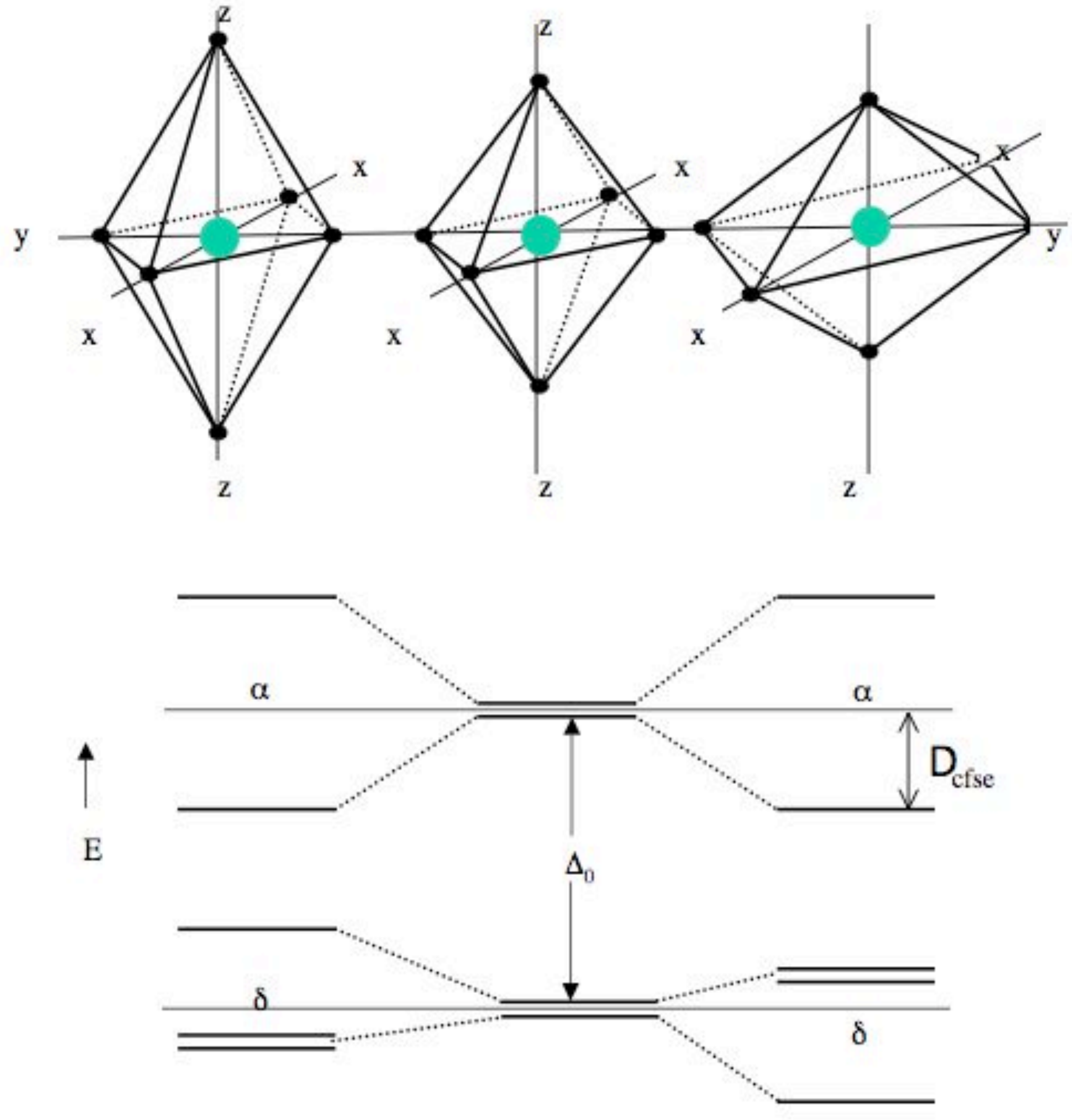

- A system with a single electron (or hole) in a degenerate level will tend to distort spontaneously.
- The effect is particularly strong for d^4 and d^9 ions in octahedral symmetry (Mn^{3+}, Cu^{2+}) which can lower their energy by distorting the crystal environment- this is the *Jahn-Teller* effect.
- If the local strain is ε, the energy change is

$$\delta E = -A\varepsilon + B\varepsilon^2.$$

where the first term is the crystal field stabilization energy and the second term is the increased elastic energy.

- The Jahn-Teller distortion may be static or dynamic.

3.2.3 High and low spin states

An ion is in a high spin state or a low spin state depending on whether the Coulomb interaction U_H leading to Hund's first rule (maximize S) is greater than or less than the crystal field splitting Δ_{cf}.

Consider a $3d^6$ ion such as Fe^{3+}.

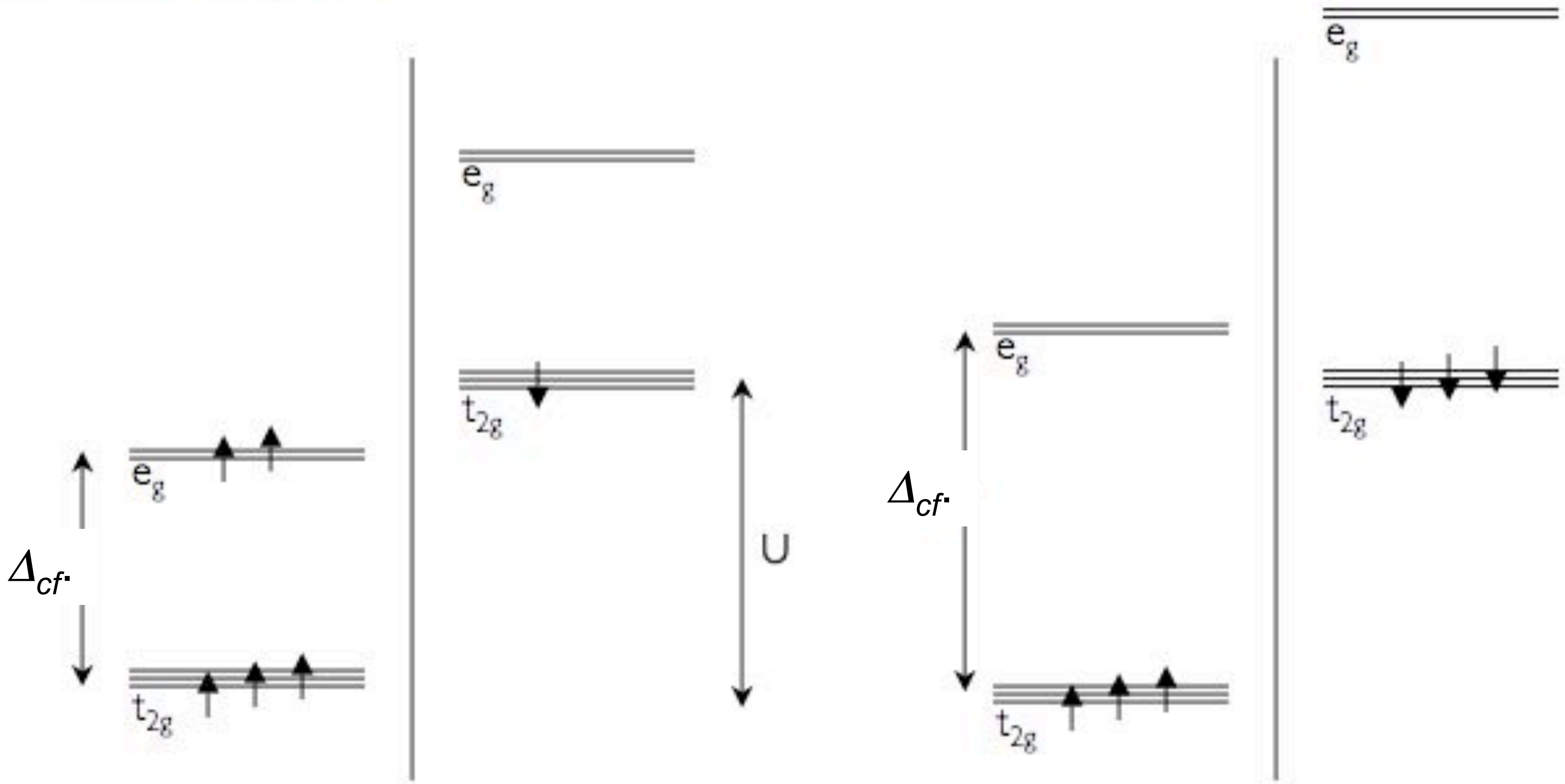

$U_H > \Delta_{cf}$. gives a high-spin state, $S = 2$ e.g. $FeCl_2$ $U_H < \Delta_{cf}$. gives a low-spin state, $S = 0$ e.g. Pyrite FeS_2

3.3 Many-electron States

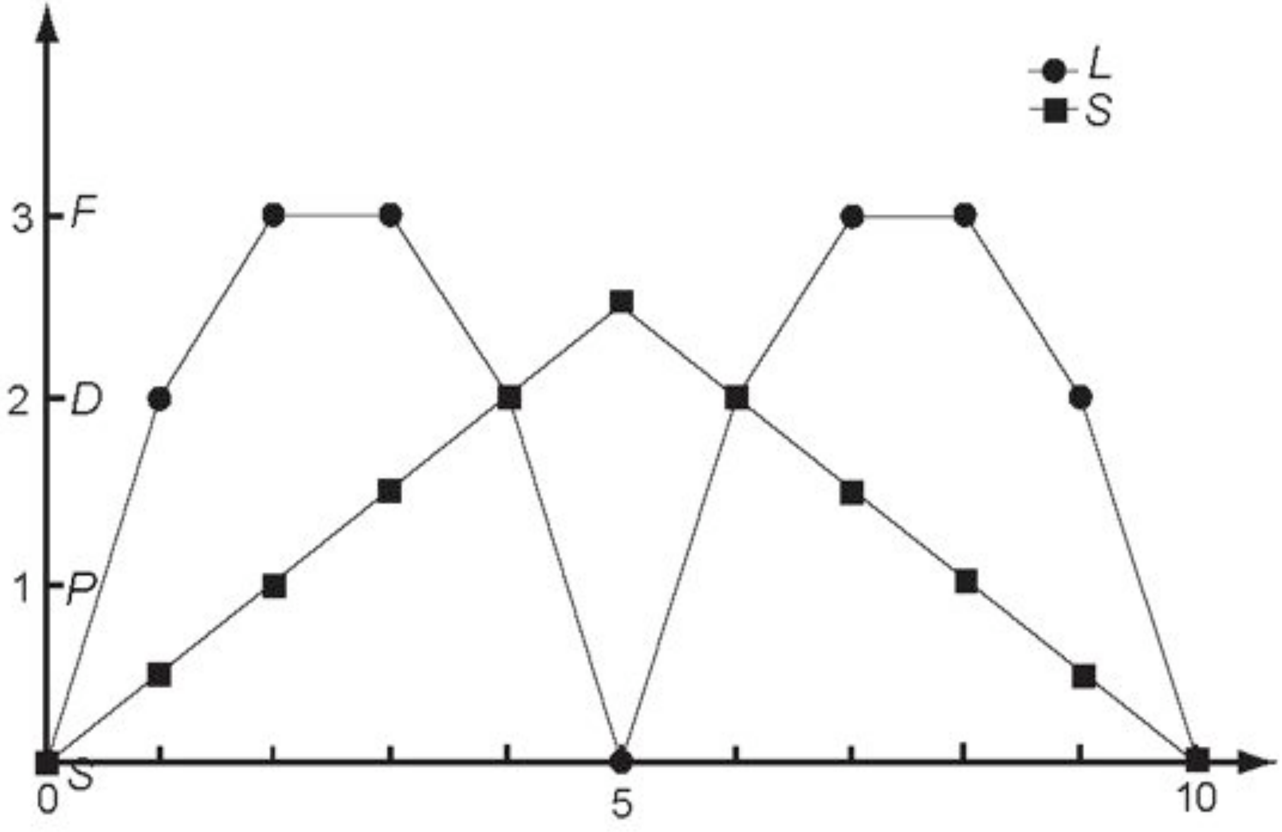

The 3*d* ions are in an S, D or F state, depending on whether L - 0, 2 or 3

3.3.1 Electronic structure of oxides

The 3d shell typically has integral occupancy $3d^n$. The 3d band is narrow, and lies in the 2p(O) -4s(M) gap 2 – 6 eV. The Fermi level lies in the d-band.

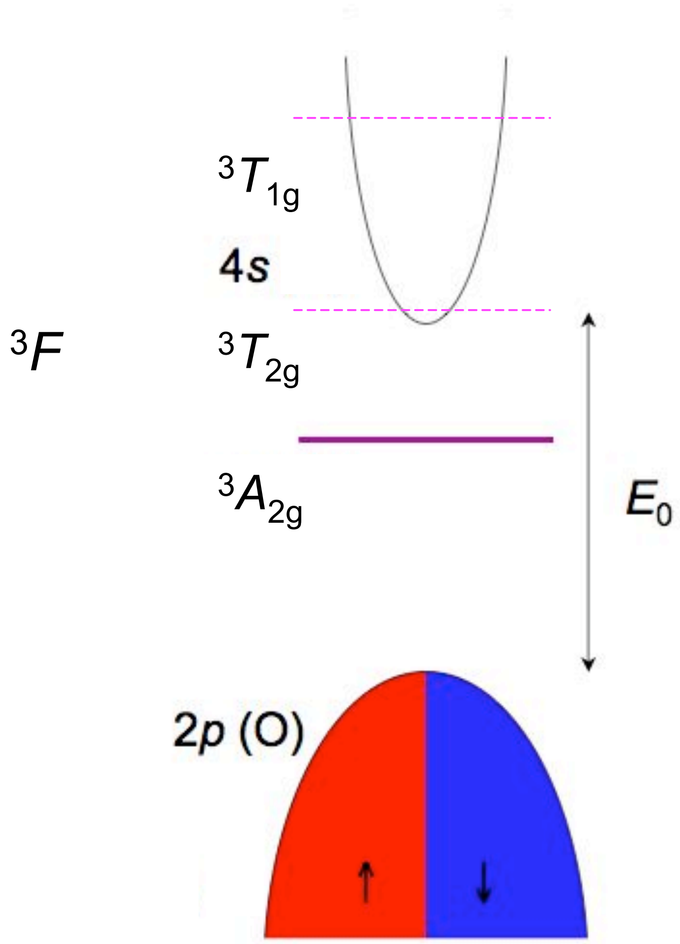

Example NiO

In insulators, the electrons in an unfilled shell interact strongly with each other giving rise to a series of sharp energy levels which are determined by the action of the crystal field on the orbital terms of the free atom. The spacing of theses levels may be determined by spectroscopy, and the crystal-field determined.

Orgel Diagrams

These diagrams show the effect of a cubic crystal field on the Hund's rule ground state term. Since a half-filled shell has spherical symmetry, the cases d^n and d^{5+n} are equivalent. Also, since a hole is the absence of an electron, the cases d^n and d^{10-n} are related.

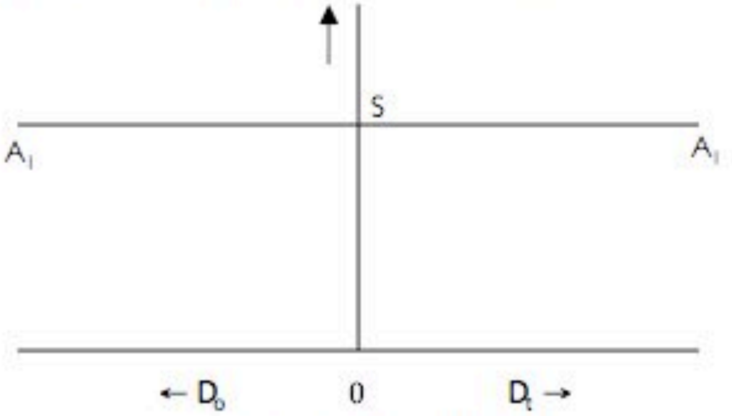

d^5 octahedral or tetrahedral

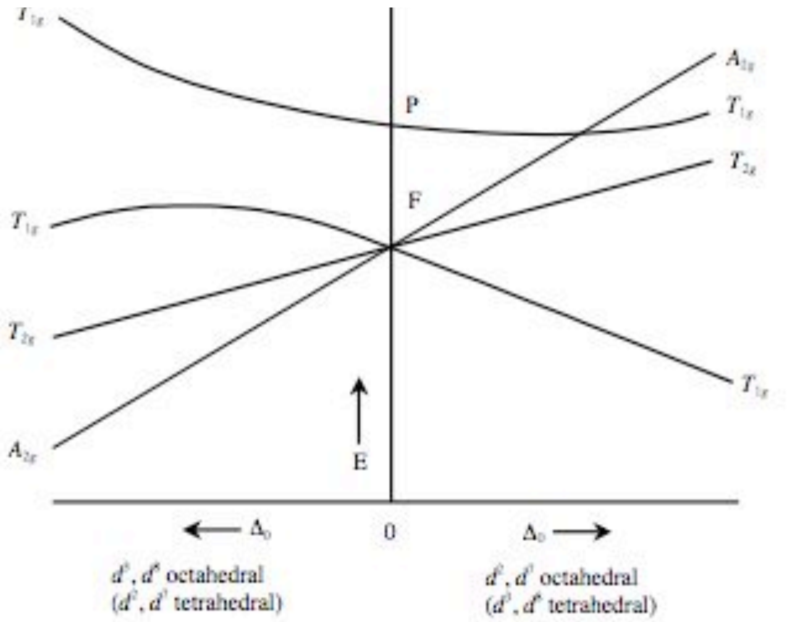

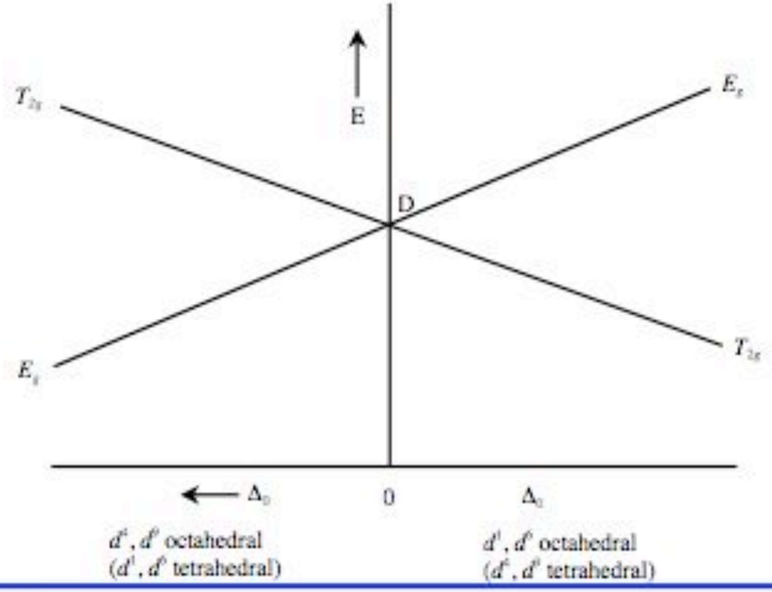

These show the splitting of the ground state and higher terms by the crystal field.
The high-spin → low-spin crossover is seen. Diagrams shown are for d-ions in octahedral environments.

d^6

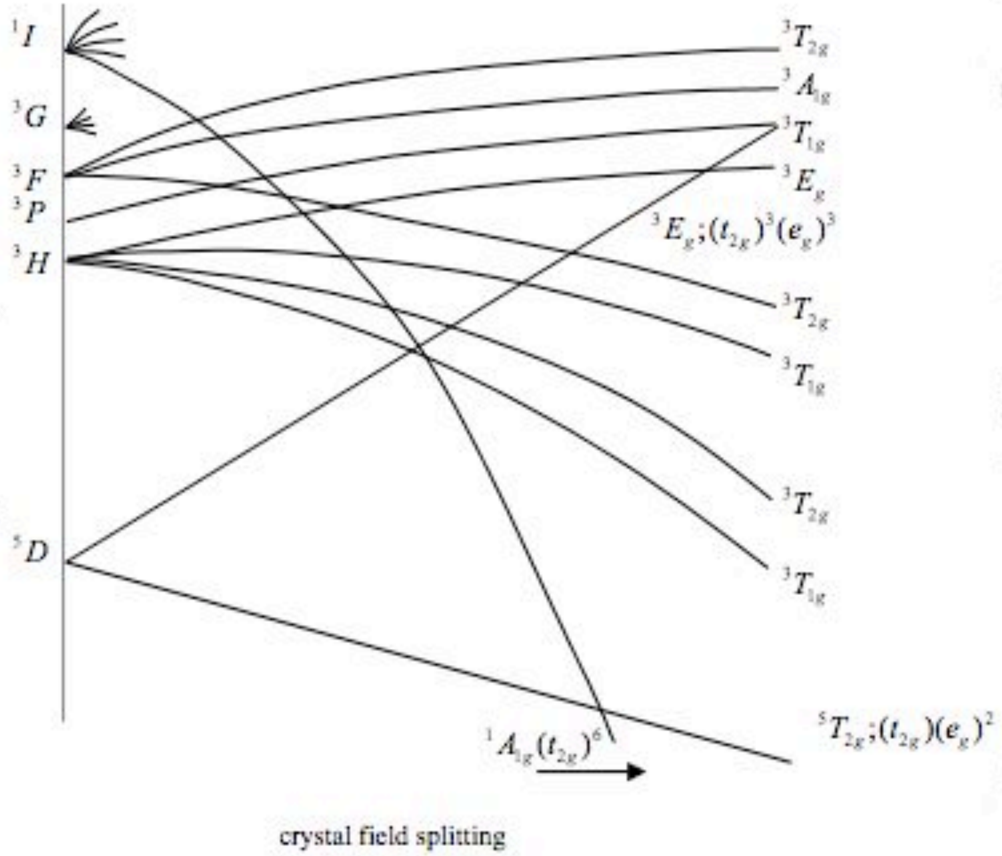

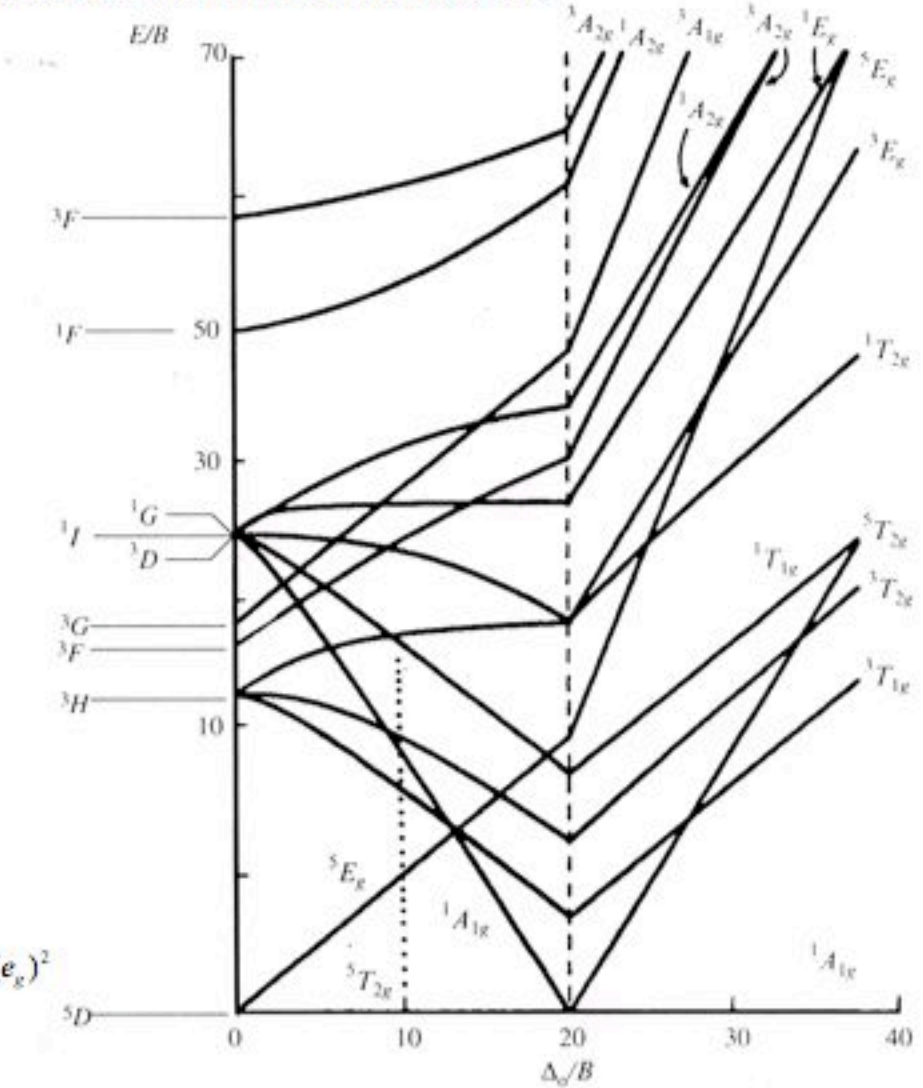

Redrawn, with the ground state at zero energy

d^5

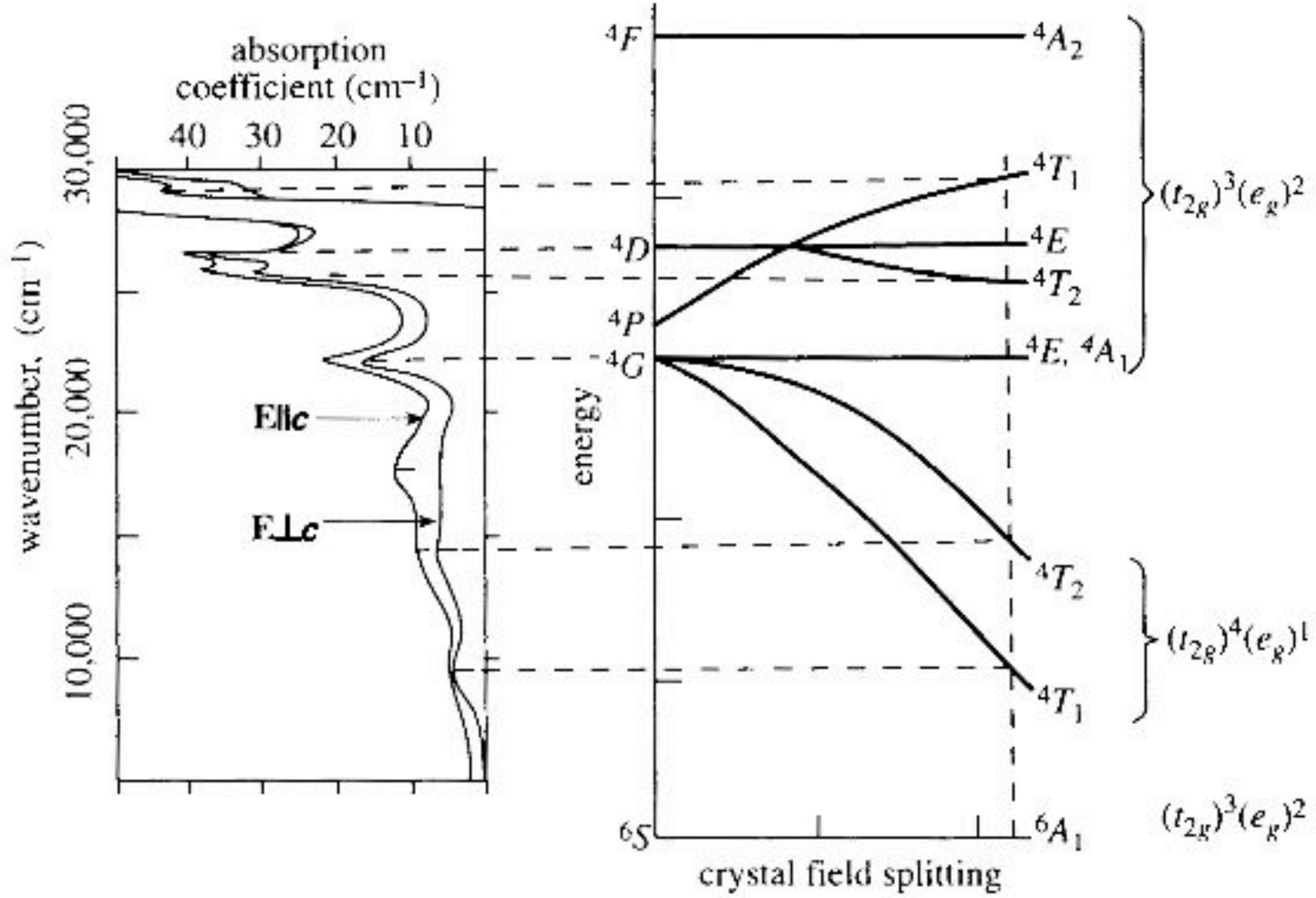

Matching the optical absorption spectrum of Fe^{3+}-doped Al_2O_3 with the calculated Tanabe-Sunago energy-level diagram to determine the crystal-field splitting at octahedral sites.

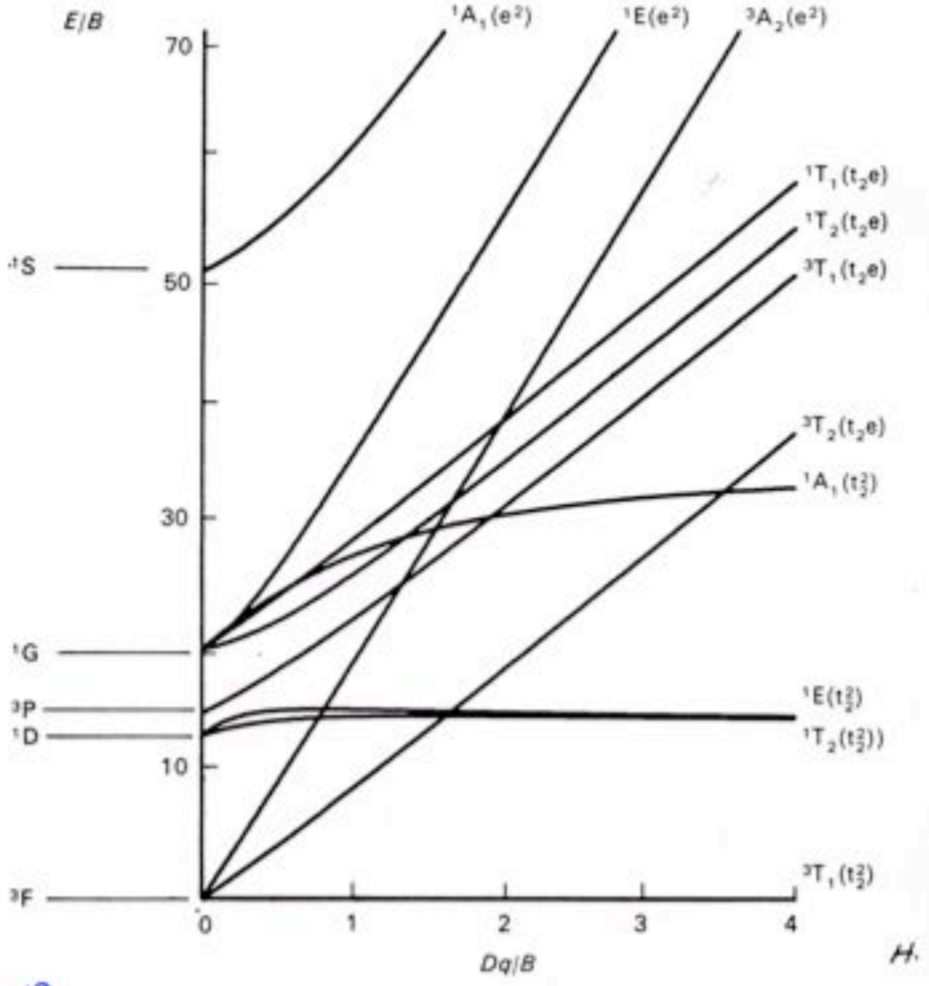

d^2

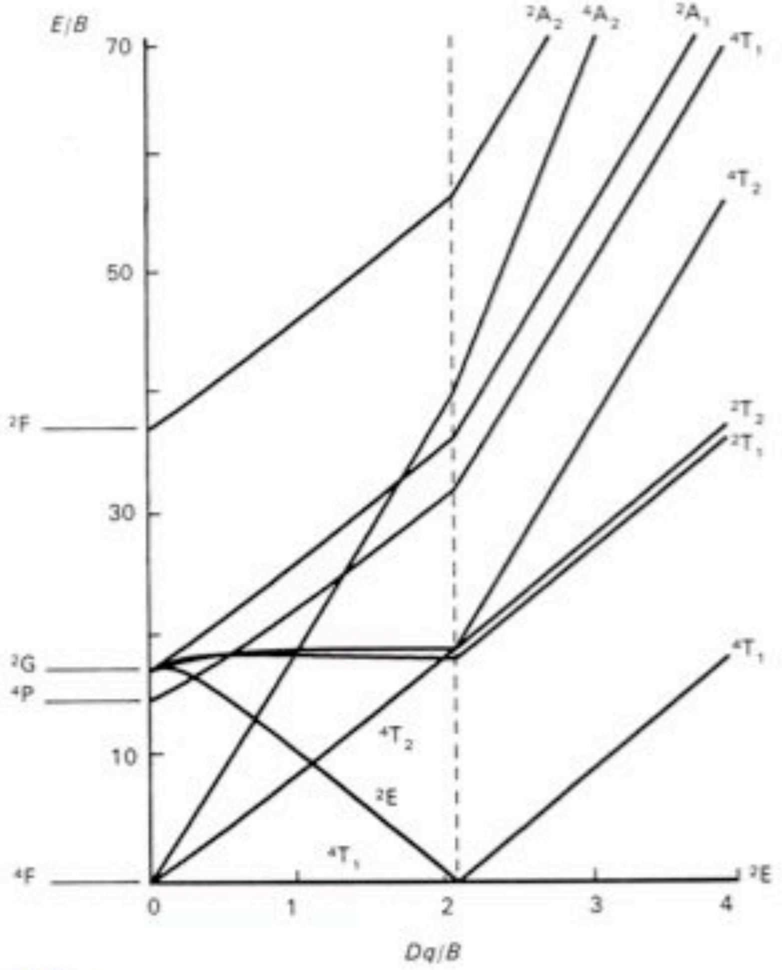

d^7

Note the similarities between the Tunabe-Sunago diagrams for d^2 and d^7.
The differences are associated with the possible low-spin states for d^7 (e.g Co^{2+}).

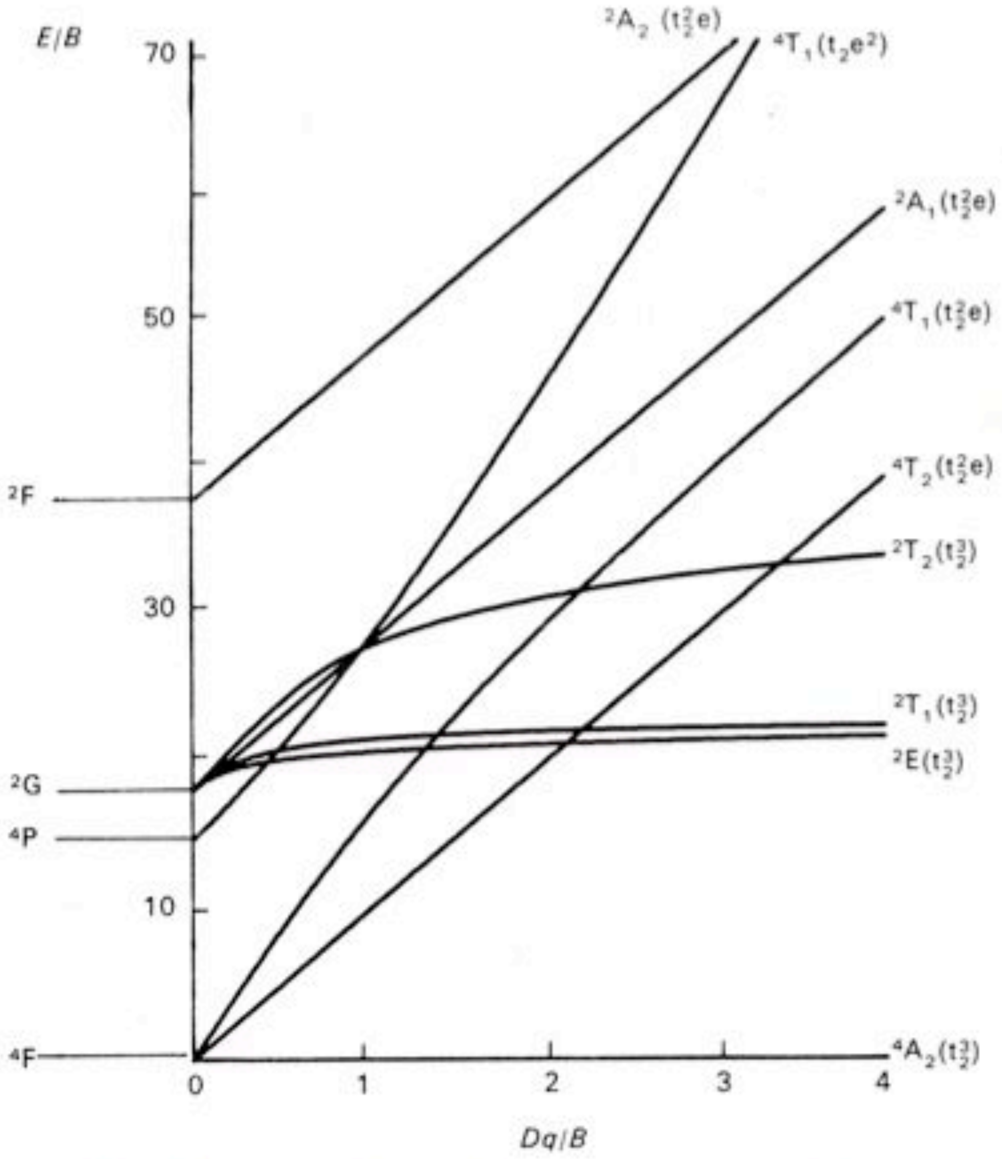

d^3

For Cr^{3+} in Al_2O_3, the cf parameter Dq/B is 2.8

3.4 Crystal Field Hamiltonian

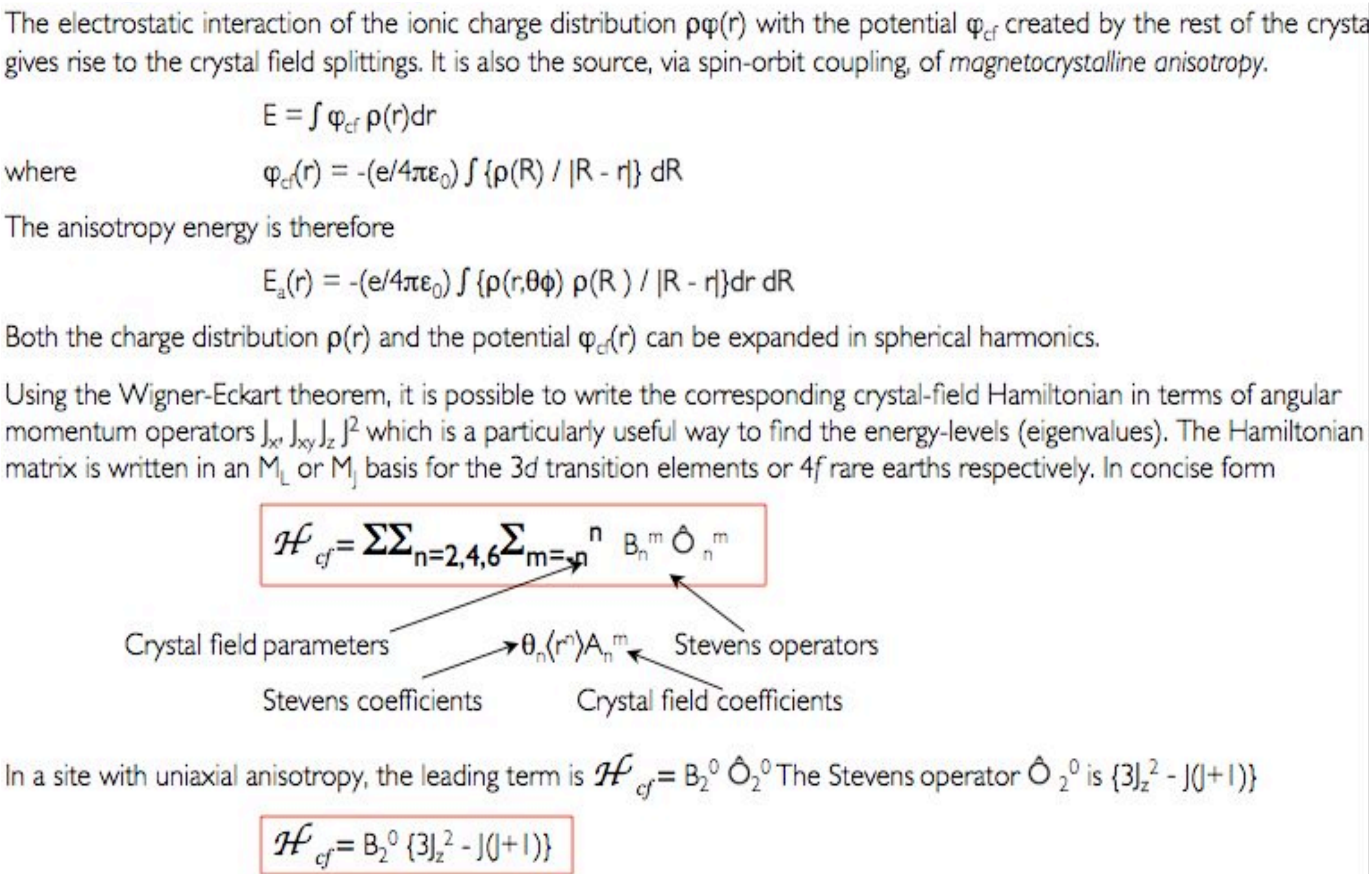

The electrostatic interaction of the ionic charge distribution ρφ(r) with the potential φ_{cf} created by the rest of the crysta gives rise to the crystal field splittings. It is also the source, via spin-orbit coupling, of *magnetocrystalline anisotropy*.

$$E = \int \varphi_{cf}\, \rho(r) dr$$

where $\varphi_{cf}(r) = -(e/4\pi\varepsilon_0) \int \{\rho(R) / |R - r|\}\, dR$

The anisotropy energy is therefore

$$E_a(r) = -(e/4\pi\varepsilon_0) \int \{\rho(r,\theta\phi)\, \rho(R) / |R - r|\} dr\, dR$$

Both the charge distribution ρ(r) and the potential $\varphi_{cf}(r)$ can be expanded in spherical harmonics.

Using the Wigner-Eckart theorem, it is possible to write the corresponding crystal-field Hamiltonian in terms of angular momentum operators J_x, J_{xy} J_z J^2 which is a particularly useful way to find the energy-levels (eigenvalues). The Hamiltonian matrix is written in an M_L or M_J basis for the 3*d* transition elements or 4*f* rare earths respectively. In concise form

$$\boxed{\mathcal{H}_{cf} = \Sigma\Sigma_{n=2,4,6}\Sigma_{m=n}^{n}\ B_n^m\, \hat{O}_n^m}$$

Crystal field parameters

$\theta_n \langle r^n \rangle A_n^m$

Stevens operators

Stevens coefficients

Crystal field coefficients

In a site with uniaxial anisotropy, the leading term is $\mathcal{H}_{cf} = B_2^0\, \hat{O}_2^0$ The Stevens operator $\hat{O}_2^0$ is $\{3J_z^2 - J(J+1)\}$

$$\boxed{\mathcal{H}_{cf} = B_2^0\, \{3J_z^2 - J(J+1)\}}$$

3.4 Crystal Field Hamiltonian

$$\boxed{\mathcal{H}_{cf} = \int \rho_0(\boldsymbol{r})\varphi_{cf}(\boldsymbol{r})\mathrm{d}^3 r.}$$

Charge distribution of the ion

potential created by the crystal

$$\varphi_{cf}(\boldsymbol{r}) = \int \frac{\rho(\mathbf{r}')}{4\pi\epsilon_0|\boldsymbol{r}-\boldsymbol{r}'|}\mathrm{d}^3 r'.$$

Here $1/|\boldsymbol{r}-\boldsymbol{r}'|$ can be expanded spherical harmonics using spherical polar coordinates $\boldsymbol{r} = (r, \theta, \phi)$ and $\boldsymbol{r}' = (r', \theta', \phi')$:

$$\frac{1}{|\boldsymbol{r}-\boldsymbol{r}'|} = \frac{1}{r'}\sum_{n=0}^{\infty}\frac{4\pi}{(2n+1)}\left(\frac{r}{r'}\right)^n \sum_{m=-\mathrm{n}}^{n}(-1)^m Y_n^{-m}(\theta', \phi')Y_n^m(\theta, \phi).$$

Hence

$$\varphi_{cf}(r, \theta, \phi) = \sum_{n=0}^{\infty}\sum_{m=-n}^{n} r^n \gamma_{nm} Y_n^m(\theta, \phi),$$

where

$$\gamma_{nm} = \frac{4\pi}{(2n+1)}\int \frac{\rho(r')(-1)^m Y_n^{-m}(\theta', \phi')}{r'^{n+1}}\mathrm{d}^3 r'.$$

structural parameters

The approximation made so far is *terrible.*It ignores the screening of the potential by the outer shells of the 4*f* ion for example, and also the covalent contribution. *But it captures the symmetry of the problem.* We proceed with it, but treat the crystal field coefficients as empirical parameters.

It is useful to expand the charge distribution of a central *4f ion* in terms of the 2^n-pole moments of the charge distribution, n = 2, 4, 6

The quadrupole moment

$$Q_2 = \int \rho_{4f}(r)(3\cos^2\theta - 1)r^2 d^3r.$$

The hexadecapole moment

$$Q_4 = \int \rho_{4f}(r)(35\cos^4\theta - 30cos^2\theta + 3)r^4 d^3r,$$

The 64-pole moment

$$Q_6 = \int \rho_{4f}(r)(231\cos^6\theta - 315\cos^4\theta + 105\cos^2\theta - 5)r^6 d^3r.$$

Rare earth quadrupole moments

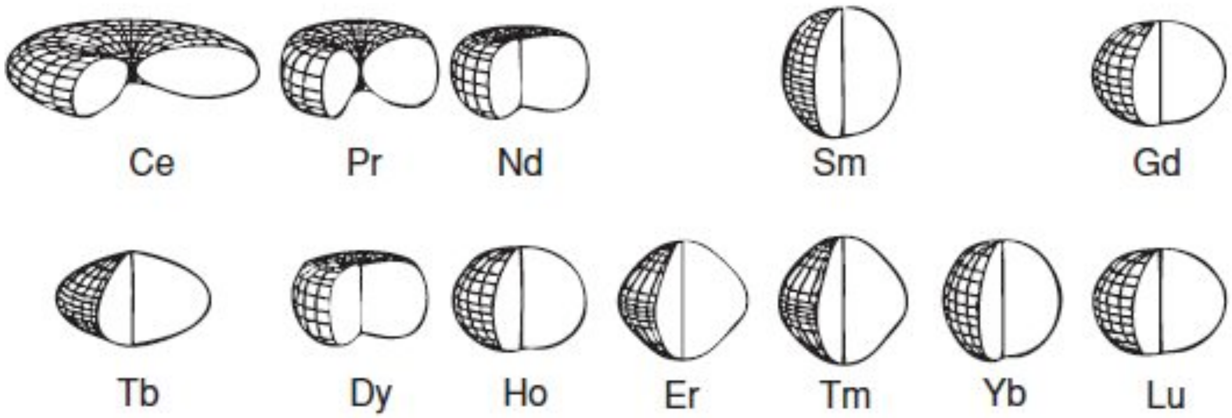

3.5 Single-ion anisotropy

Single-ion anisotropy is due to the electrostatic crystal field interaction + spin-orbit interaction. The 4f charge distribution $\rho_0(\mathbf{r})$ interacts with the crystal field potential $\varphi_{cf}(\mathbf{r})$ to stabilizes some particular orbitals; spin-orbit interaction $-\Lambda \boldsymbol{L}.\boldsymbol{S}$ then leads to magnetic moment alignment along some specific directions in the crystal.

The leading term in the crystal field interaction is

$$\varepsilon_a = (1/2) Q_2 A_2^0 (3\cos^2\theta - 1),$$

where A_2^0 is the uniaxial second-order crystal field parameter, which described the electric field gradient created by the crystal which interacts with the 4*f* quadrupole moment.

The crystal field interaction can be expressed in terms of angular momentum operators, using the Wigner-Eckart theorem

$$\boxed{\mathcal{H}_{cf} = \sum_{n=0,2,4,6} \sum_{m=-n,\dots,n} B_n^m \hat{O}_n^m ,}$$

cf coefficient

Stevens operators

Here $B_n^m = \theta_n \langle r_{4f}^n \rangle A_n^m$ and θ_n is different for each 4*f* ion, proportional to the 2^n-pole moment

$Q_2 = 2\,\theta_2\langle r_{4f}^2\rangle$ $Q_4 = 8\,\theta_4\langle r_{4f}^4\rangle$ $Q_6 = 16\,\theta_6\langle r_{4f}^6\rangle$

$A_n^m \sim \gamma_{nm}$ parameterises the crystal field produced by the lattice.

NB. $Q_2 \neq 0$ for J (or L) ≥ 1

$Q_4 \neq 0$ for J (or L) ≥ 2

$Q_6 \neq 0$ for J (or L) ≥ 3

The Stevens operators are tabulated, as well as which ones feature in each point symmetry

e.g. The leading term in any uniaxial site is the one in O_2^0

$$\hat{\mathbf{O}}_2^0 = [3\hat{J}_z^2 - J(J+1)].$$

The complete second order (uniaxial) cf Hamiltonian is

$$\mathcal{H}_{cf} = \theta_2 \langle r_{4f}^2 \rangle \left[A_2^0 \hat{\mathbf{O}}_2^0 + A_2^2 \hat{\mathbf{O}}_2^{2(c)} \right]$$

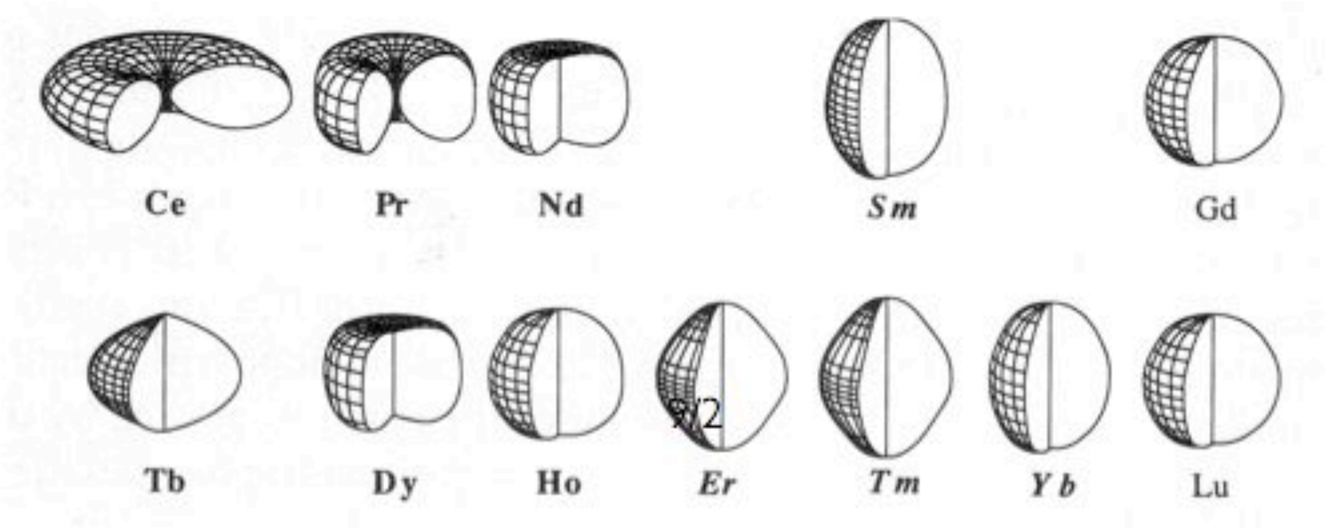

Charge distributions of the rare-earth ions. Those with a positive quadrupole moment ($\theta_2 > 0$), italic type distinguished from those with a negative quadrupole moment ($\theta_2 < 0$) bold type. Note the quarter-shell changes,

e.g. Nd^{3+} J = 9/2

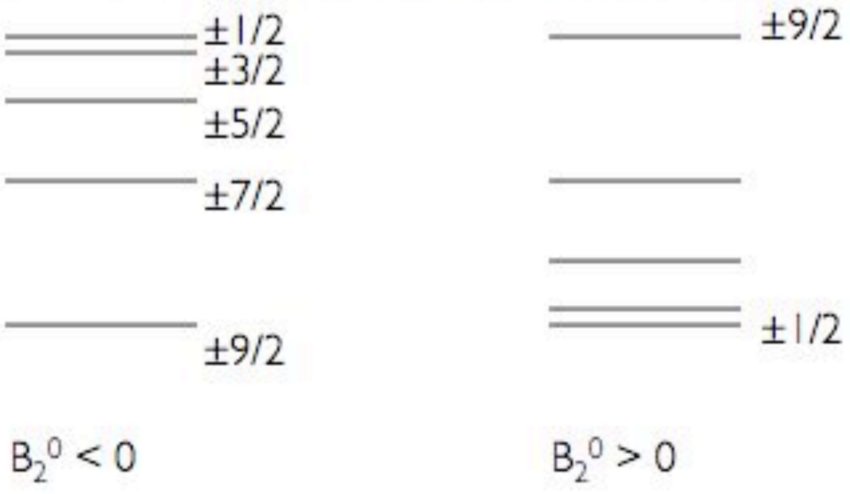

The cf Hamiltonian for a site with cubic symmetry is

$$\mathcal{H}_{cf} = \theta_4 \langle r_{4f}^4 \rangle \left[A_4^0 \hat{O}_4^0 + 5 A_4^{4(c)} \hat{O}_2^{2(c)} \right] + \theta_6 \langle r_{4f}^6 \rangle \left[A_6^0 \hat{O}_6^0 - 21 A_6^0 \hat{O}_2^{2(c)} \right]$$

For 3*d* ions only the fourth-order terms exist; (l = 2)

Kramer’s theorem

It follows from time-reversal symmetry that the cf energy levels of any ion with an odd number of electrons, and therefore half-integral angular momentum, must be at least 2-fold degenerate. These are the $|\pm M_J\rangle$ Kramers doublets.

When J is integral, ther will be a $|0\rangle$ singlet (with no magnetic moment) and a series of doublets.

Basic Concepts in Magnetism

J. M. D. Coey

School of Physics and CRANN, Trinity College Dublin

Ireland.

1. Magnetostatics
2. Magnetism of multi-electron atoms
3. Crystal field
4. Magnetism of the free electron gas
5. Dilute magnetic oxides

Comments and corrections please: jcoey@tcd.ie www.tcd.ie/Physics/Magnetism

4. Magnetism of free electrons

4.1 Localized and delocalized electrons

LOCALIZED MAGNETISM

Integral number of 3d or 4f electrons on the ion core; Integral number of unpaired spins; Discreet energy levels.

Ni^{2+} 3d^{8} $m = 2\ \mu_B$

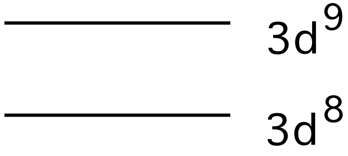

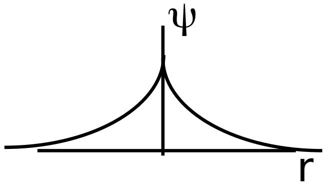

$\psi \approx \exp(-r/a_0)$

Boltzmann statistics

DELOCALIZED MAGNETISM

Nonintegral number of unpaired spins per atom.

Spin-polarized energy bands with strong correlations.

Ni 3d$^{9.4}$4s$^{0.6}$ $m = 0.6\ \mu_B$

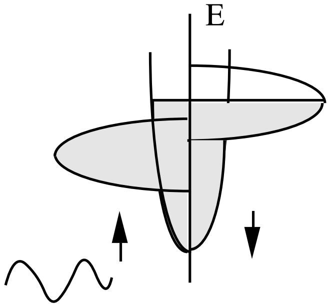

$\psi \approx \exp(-i\mathbf{k}.\mathbf{r})$

Fermi-Dirac statistics

4f metals	*localized electrons*
4f compounds	*localized electrons*
3d compounds	*localized/delocalized electrons*
3d metals	*delocalized electrons.*

Above the Curie temperature, neither localized nor delocalized moments disappear, they just become disordered in the paramagnetic state, $T > T_C$.

Cyclotron orbits

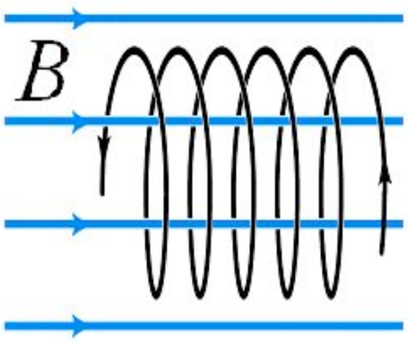

Free electrons follow cyclotron orbits in a magnetic field. Electron has velocity ***v*** then it experiences a Lorentz force

$$\boxed{\boldsymbol{F} = -e\boldsymbol{v} \times \boldsymbol{B}}$$

The electron executes circular motion about the direction of ***B*** (tracing a helical path if $v_{||} \neq 0$)

Cyclotron frequency $f_c = v_{\perp}/2\pi r$

$$\boxed{f_c = eB/2\pi m_e}$$

Electrons in cyclotron orbits radiate at the cyclotron frequency

Examples: — ESRF
— Microwave oven

Larmor precession

Bound electrons undergo Larmor precession.
If an electron is constrained to an orbit it has an associated magnetic moment $\boldsymbol{m} = \gamma \boldsymbol{l}$ which experiences a torque

$$\boldsymbol{\Gamma} = \boldsymbol{m} \times \mathbf{B} = d\boldsymbol{l}/dt$$

perpendicular to the direction of $\boldsymbol{m}$.
Thus $\boldsymbol{m}$ precesses about the applied field direction at the Larmor frequency

$$\boxed{f_L = \gamma B/2\pi}$$

Since $\gamma_e = -(e/m_e)$, the cyclotron and Larmor frequencies are the *same* for electrons; 28.0 GHz T^{-1}

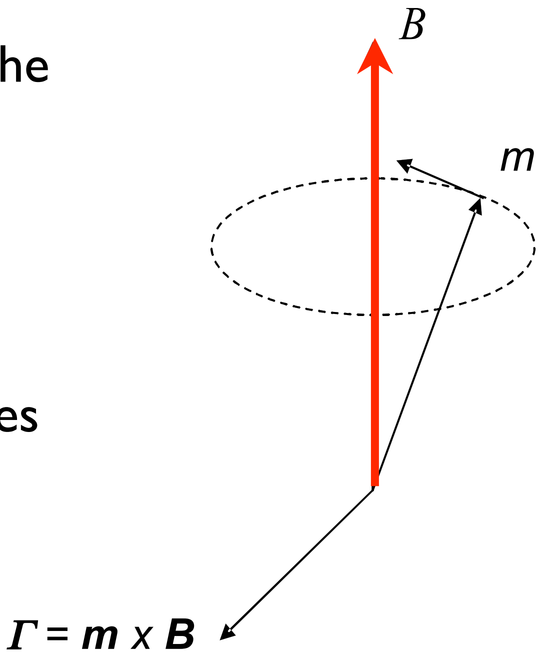

5.2 The free electron model

Simplest model for conduction electrons in a solid. Works well for weakly-correlated electrons in broad bands, especially *s*-band metals such as copper $3d^{10}4s^1$

Hamiltonian for the electrons confined in a box of sides L.

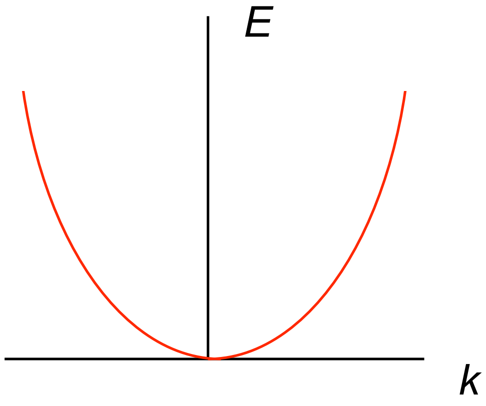

$$\boxed{H = \boldsymbol{p}^2/2m_e + V(\boldsymbol{r})}$$

Schrodinger's equation: $-(\hbar^2/2m_e)\nabla^2\psi = (E-V)\psi$

Solutions are free-electron waves $\psi = L^{-3/2}\exp(i\mathbf{k}.\mathbf{r})$

Momentum: $\mathbf{p} = -i\hbar\nabla = \hbar\mathbf{k}$ Energy: $E = \hbar^2k^2/2m_e$

Allowed values $k_i = \pm 2\pi n_i/L$, n_i is an integer

2 electrons per state/point in *k*-space (spin degeneracy).

Each state occupies a volume $(2\pi/L)^3$

N electrons occupy a volume of $(N/2)(2\pi/L)^3$

At $T = 0$ electrons occupy lowest available energy states: Highest occupied states are at the Fermi energy.

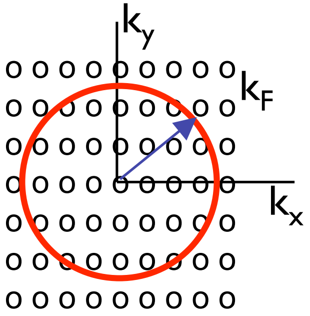

$$\boxed{\epsilon_F = \hbar^2 k_F^2/2m_e}$$

Occupied states fill a sphere of volume: $(4/3)\pi k_F^3 = 2N(2\pi/L)^3$

Fermi wavevector $\boxed{k_F = (3\pi^2 n)^{1/3}}$

($n = N/L^3$ is electron density)

The spherical Fermi surface of radius k_F separates the occupied and unoccupied states.

The Fermi surface of copper.

Density of states; $\mathcal{D}_{\uparrow,\downarrow}(\varepsilon) = (1/2)dn/d\varepsilon = (1/4\pi^2)(2m_e/\hbar^2)^{3/2}\,\varepsilon^{1/2}$ for either spin.

Density of states at the Fermi Level:

$$\boxed{\mathcal{D}_{\uparrow,\downarrow}(\varepsilon_F) = 3n/4\varepsilon_F}$$

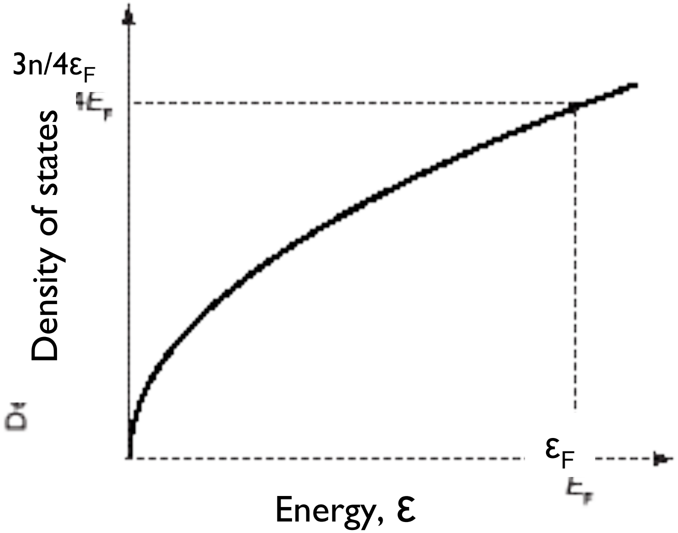

Electrons moving in a crystalline solids's lattice experience a periodic potential.

Bloch's theorem: $\boxed{\psi(\mathbf{r}) \approx \exp(i\mathbf{k}.\mathbf{r})u_k(\mathbf{r})}$

where $u_k(\mathbf{r})$ has the periodicity of the lattice.

If the Bragg condition $2\boldsymbol{k}.\boldsymbol{G} = G^2$ is satisfied, reflection of the electron waves at the Brillouin zone boundaries leads to sharp structure and gaps in the DOS

The free electron model can be extended to systems with non-parabolic DOS by defining an effective electron mass $m_e^* = \hbar^2(\partial^2\varepsilon/\partial k^2)^{-1}$ which represents the effect of the lattice potential on the electrons.

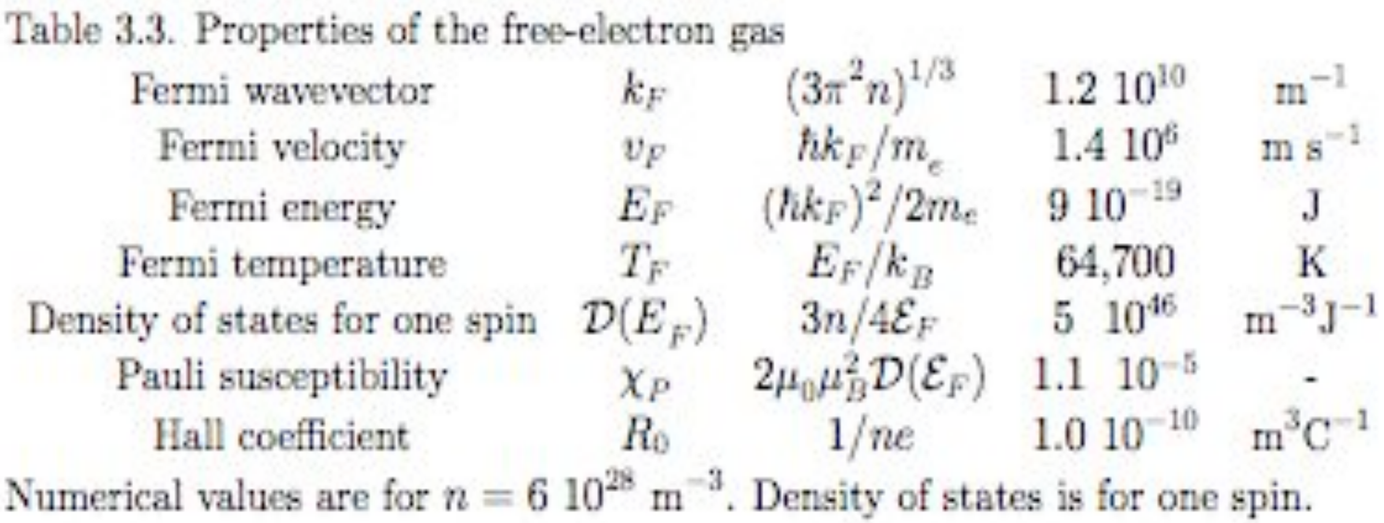

Table 3.3. Properties of the free-electron gas

Fermi wavevector	k_F	$(3\pi^2 n)^{1/3}$	$1.2\ 10^{10}$	m^{-1}
Fermi velocity	v_F	$\hbar k_F/m_e$	$1.4\ 10^{6}$	$\mathrm{m\ s}^{-1}$
Fermi energy	E_F	$(\hbar k_F)^2/2m_e$	$9\ 10^{-19}$	J
Fermi temperature	T_F	E_F/k_B	64,700	K
Density of states for one spin	$\mathcal{D}(E_F)$	$3n/4\mathcal{E}_F$	$5\ \ 10^{46}$	$\mathrm{m}^{-3}\mathrm{J}^{-1}$
Pauli susceptibility	χ_P	$2\mu_0\mu_B^2\mathcal{D}(\mathcal{E}_F)$	$1.1\ \ 10^{-5}$	-
Hall coefficient	R_0	$1/ne$	$1.0\ 10^{-10}$	$\mathrm{m}^3\mathrm{C}^{-1}$

Numerical values are for $n = 6\ 10^{28}\ \mathrm{m}^{-3}$. Density of states is for one spin.

$$f(\mathcal{E}) = \frac{1}{\{\exp[(\mathcal{E}-\mu)/k_B T] + 1\}}$$

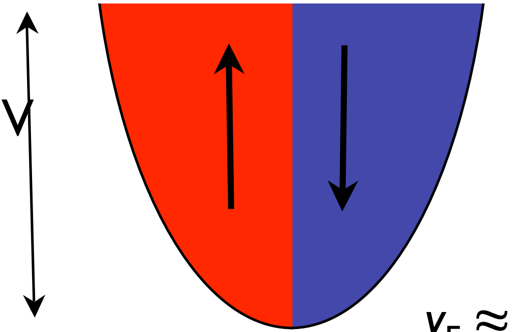

$E_F \approx 6$ eV

$v_F \approx 1.4\ 10^6\ \mathrm{m\ s}^{-1}$

$k_F \approx 1.2\ 10^{10}\ \mathrm{m}^{-1}$

5.3 Spin moment and susceptibility - band electrons

The calculation for metals proceeds on a quite different basis. The electrons are indistinguishable particles which obey Fermi-Dirac statistics. They are not localized, so Boltzmann statistics cannot be applied. The electrons have s = 1/2, $\mathcal{m} = \mu_B$. They partly-fill some energy band up to the Fermi level E_F.

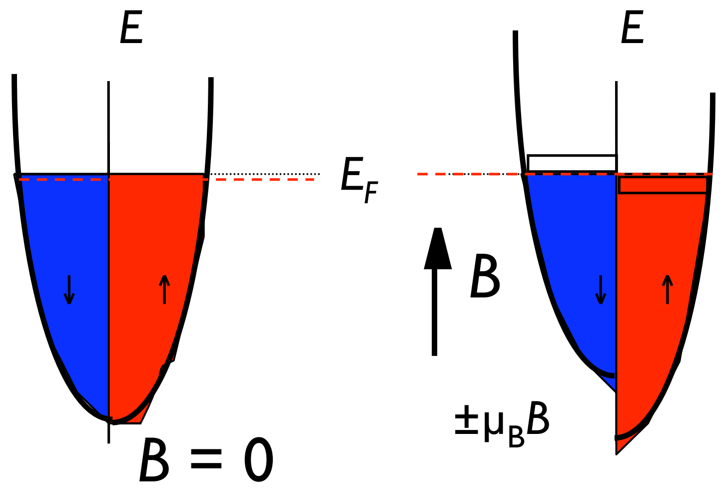

A rough calculation gives the susceptibility as follows:

$$\chi = (N^{\uparrow} - N^{\downarrow})\mu_B/H$$

$$\approx 2[\mathcal{D}(E_F)\mu_0 g\mu_B H]\mu_B/H$$ where $\mathcal{D}(E_F)$ is the density of states at the Fermi level for one spin direction.

$$\boxed{\chi_{Pauli} \approx 2\mu_0\, \mathcal{D}(E_F)\mu_B^2}$$

This is known as the *Pauli* susceptibility. Unlike the Curie susceptibility, it is very small, and temperature independent.

The density of states $N(E_F)$ in a band is approximately N/2W, where W is the bandwidth (which is typically a few eV). Comparing the expression for the Pauli susceptibility with that for the Curie susceptibility $\chi_{curie} = \mu_0 N\mu_B^2/k_BT$, we see that the Pauli susceptibility is a factor k_BT/W smaller than the Curie susceptibility . The factor is of order 100 at room temperature. χ_{Pauli} is of order 10^{-5}.

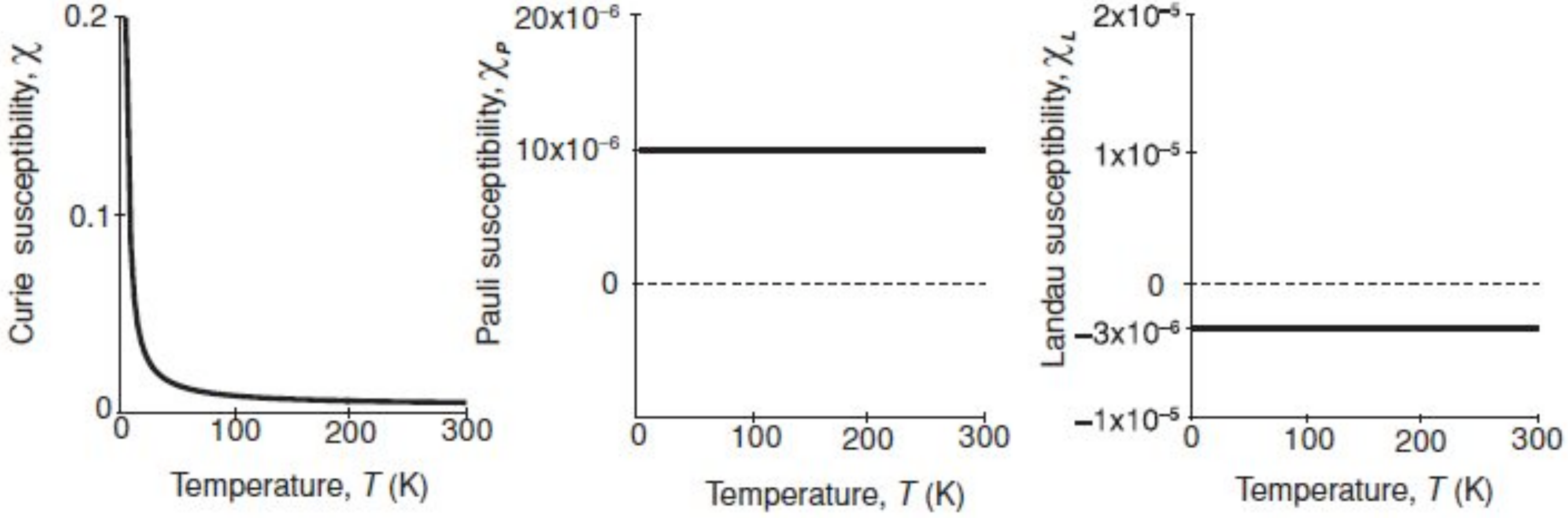
Curie susceptibility, χ
0.2
0.1
0
0
100
200
300
Temperature, T (K)
Pauli susceptibility, χ_P
20x10^{-6}
10x10^{-6}
0
0
100
200
300
Temperature, T (K)
Landau susceptibility, χ_L
2x10^{-5}
1x10^{-5}
0
−3x10^{-6}
−1x10^{-5}
0
100
200
300
Temperature, T (K)

Some metals have narrow bands and a large density of states at the Fermi level; In this case it is possible for the band to split *spontaneously*, and for ferromagnetism or antiferromagnetism to appear.

metal	order	$m(\mu_B)$
Cr	af	0.6
Mn	af	1.0
Fe	ferro	2.2
Co	ferro	1.7
Ni	ferri	0.6

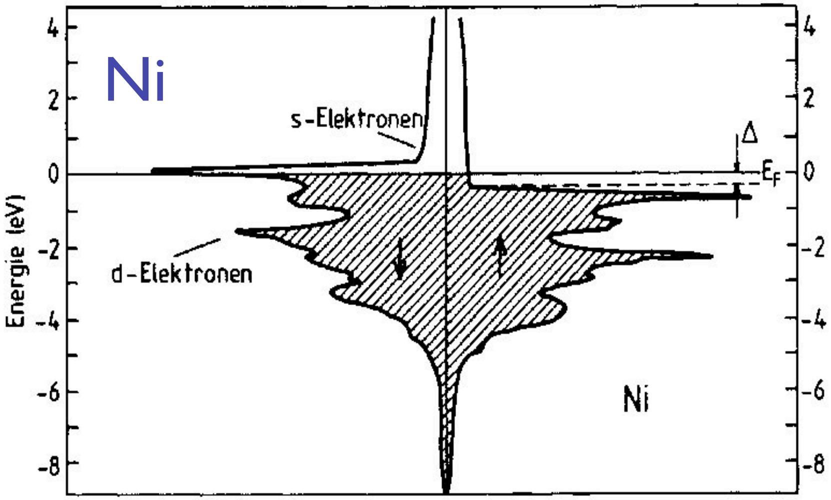

Strong ferromagnets like Co or Ni have all the states in the ↑ d-band filled (5 per atom).

Weak ferromagnets like Fe have both ↑ and ↓ d-electrons at the E_F.

3-d solid

$\mathcal{D}(\varepsilon) \propto \varepsilon^{1/2}$

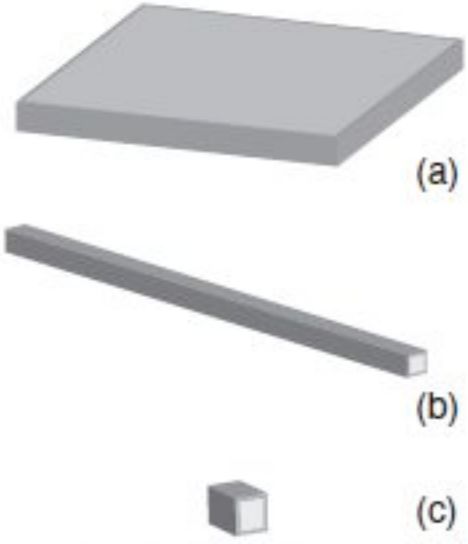

$\mathcal{D}(\varepsilon)$ = constant

$\mathcal{D}(\varepsilon) \propto \varepsilon^{-1/2}$

Discreet levels

Confinement of the free-electron gas: (a) in two dimensions, (b) in one dimension – a quantum wire, and (c) in zero dimensions – a quantum dot.

5.4 Landau diamagnetism

Free electron model was used by Landau to calculate the orbital diamagnetism of conduction electrons. The result is:

$$\boxed{\chi_L = -n\mu_0\mu_B^2/2k_BT_F}$$

exactly one third of the Pauli susceptibility, and opposite in sign.

The real band structure is taken into account in an approximate way by renormalizing the electron mass. Replace m_e by an effective mass m^*

Then $\chi_L = -(1/3)(m_e/m^*)\,\chi_P$

In some semimetals such as graphite or bismuth, m^* can be $\approx 0.01\ m_e$, hence the diamagnetism of the conduction electrons may sometimes be the dominant contribution to the susceptibility. ($\chi_L = -4\ 10^{-4}$ for graphite)

Susceptibility of the elements

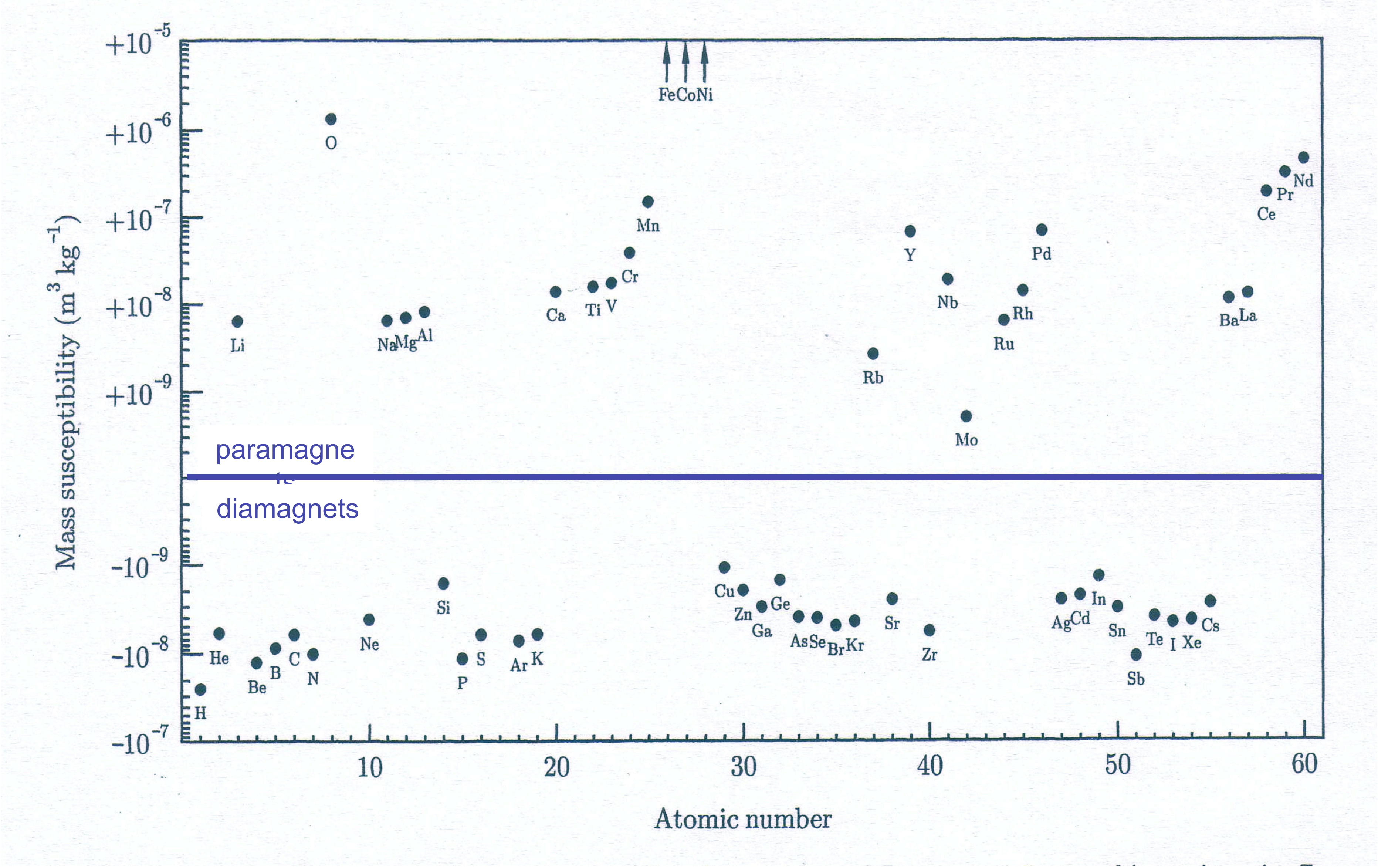

	χ 10^{-9} $\mathrm{m^3\ kg^{-1}}$		χ 10^{-9} $\mathrm{m^3\ kg^{-1}}$		χ 10^{-9} $\mathrm{m^3\ kg^{-1}}$
MgO	-3.1	C(diamond)	-6.2	Cu	1.1
Al_2O_3	-4.5	C(graphite)	$\chi_\parallel$ -6.3	Ag	2.4
TiO_2	0.9		$\chi_\perp$-138.0	Au	1.9
$SrTiO_3$		Si	-1.8	Al	7.9
ZnO	-6.2	Ge	-1.5	Ta	10.7
ZrO_2	-1.1	NaCl	-6.4	Zn	-2.2
HfO_2	-1.4	GaAs		Pd	67.0
SiO_2	-7.1	GaN		Pt	12.2
$MgAl_2O_4$		InSb		In	-7.0
H_2O	-9.0	Perspex	-5.0	Bi	-17.0

5.5 Quantum oscillations

Let $B = B_z$, $\mathbf{A} = (0, xB, 0)$, $V(r) = 0$ and $m = m^*$

Schrodinger's equation $\frac{1}{2m^*}[p_x^2 + (p_y + xB)^2 + p_z^2]\psi = E\psi$

$$\psi(x)e^{ik_y y}e^{ik_z z}$$

$$\left[-\frac{\hbar^2}{2m^*}\frac{d^2}{dx^2} + \frac{1}{2}m^*\omega_c(x - x_0)^2\right]\psi(x) = E'\psi(x)$$

$\omega_c = eB/m^*$, $x_0 = -\hbar k_y/eB$ $E' = E - (\hbar^2/2m)k_z^2$

$$E' = E_n = (n+\tfrac{1}{2})\hbar\omega_c$$

$$\boxed{E = \frac{\hbar^2 k_z^2}{2m^*} + (n + \frac{1}{2})\hbar\omega_c}$$

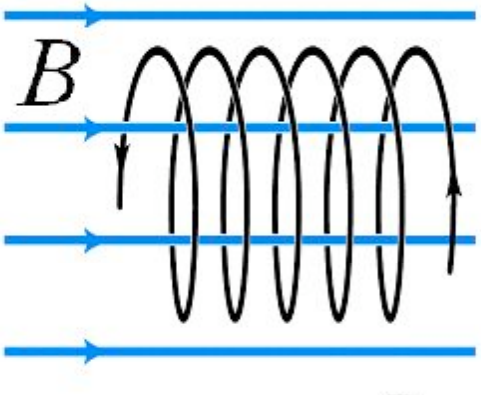

$$\omega = \frac{eB}{m_e}$$

The motion is a plane wave along Oz, plus a simple harmonic oscillation at f_c in the plane.

When a magnetic field is applied, the states in the Fermi sphere collapse onto a series of tubes. Each tube corresponds to one Landaue level (n - value). As the field increases, the tubes expand and the outer one empties periodically as field increases. An oscillatory variation in $1/B^2$ of magnetization (de Haas - van Alphen effect) or of conductivity (Shubnikov - de Haas effect) appears.

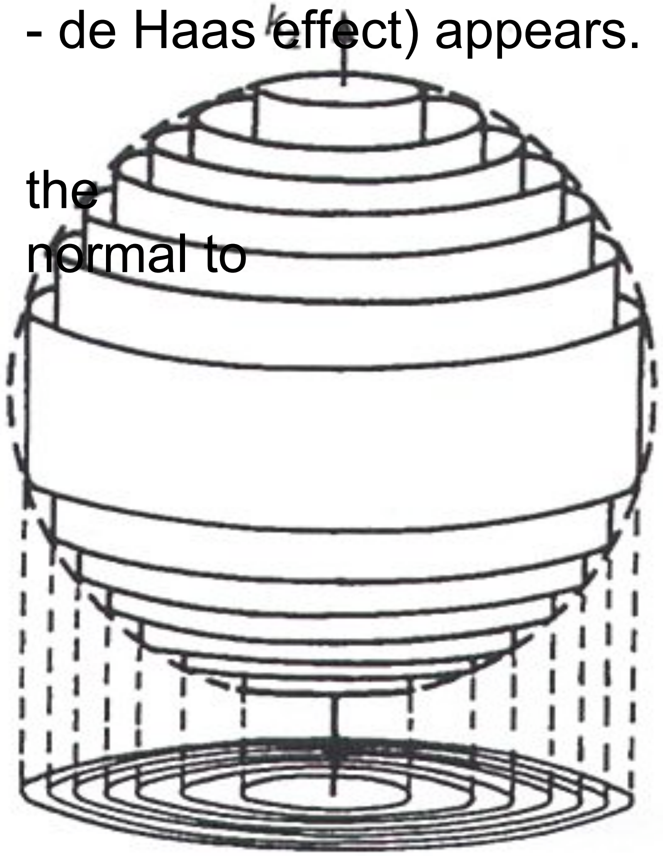

From the period, it is possible to deduce the cross section area of the Fermi surface normal to the tubes.